

Richard *SANTER*
(LISE)



**SENTINEL-3 OPTICAL PRODUCTS AND ALGORITHM
DEFINITION**
OLCI Level 2 Algorithm Theoretical Basis Document
Pixel Classification

Ref: S3-L2-SD-03-C01-LISE-ATBD
Issue: 2.3
Date: 17/07/10
Page 1 of 69

OLCI Level 2

Algorithm Theoretical Basis Document

Pixel Classification

DOCUMENT REF: S3-L2-SD-03-C01-LISE-ATBD
DELIVERABLE REF: SD-03-C
VERSION: 2.3

Document Signature Table

	Name	Function	Company	Signature	Date
Prepared	R. Santer S. Cozette	Consultant	LISE		17/07/10
Edited revision	S. Lavender	Project Manager	ARGANS Ltd		
Verified	O. Fanton d'Andon	OLCI Coordinator	ACRI-ST		
Released	S. Lavender	Project Manager	ARGANS Ltd		

Change record

Issue	Date	Description	Change pages
1.0	21/08/2009	Version 1 (PDR delivery)	
1.1	16/03/2010	Edited version based on feedback received at PDR	Rearrangement and simplification of whole document
1.2	04/04/2010	Iteration within the OLCI team	Addition of executive summary
2.0	08/04/2010	Review and acceptance of edits	Executive summary
2.1	03/05/2010	CDR RID update	
2.2	30/06/2010	Final review / updates before delta CDR release	Updated with respect to CDR ACT-76: Improved bulleted list in

			§3; corrected OLCI bands in table 2 and replaced OCLI with OLCI throughout the document.
2.3	17/07/2010	Corrections linked to delta CDR review	Updated executive summary – correct wavelength for O17; comment in legend as to why Figure 3 appears truncated (CDR-158).

Distribution List

Organisation	To
ESA	Philippe Goryl, Alessandra Buongiorno and Carla Santella
EUMETSAT	Vincent Fournier-Sicre and Vincenzo Santacesaria
CONSORTIUM PARTNERS	ARGANS, ACRI-ST, RAL, Brockmann Consult, Elsag-Datamat

Executive summary

The **OLCI** L2 classification is first the heritage of the MERIS prototype processor (MEGS8.0). Second, the main difference between MERIS and **OLCI** is the absence of an atmospheric branch in **OLCI** (cloud and aerosol over land). Therefore, the “decision” flags are driven by the possibilities to retrieve the L2 water and land parameters and the quality of these retrievals.

An evolution is to set “geophysical” flags. Over land, snow and sand flags can be introduced. Over water, a sea ice flag can be set. Another useful flag would be cloud shadow; a result of the sun beam geometry and the altitude of the cloud top (provided in MERIS by the cloud top pressure).

At L1, the land-water classification of **OLCI** should be improved thanks to better auxiliary information and to the addition of a tide map. The L2 radiometric consolidation of the land-water flag of **OLCI** will be identical to MEGS8.0.

The classification over land of **OLCI** will be in line with MEGS8.0, but with:

- (i) The high bright flag is raised if $\rho_{\text{TOA_B2}}$ above a threshold (40%, TBC); used to eliminate bright clouds, sand and snow. The low bright flag is set as for MERIS (Section 2.1).
- (ii) O12 at 761.25 nm instead of MERIS B11 at 761.75 nm (see table 2 for spectral band definition) to compute the O2 apparent pressure, P_1 . The threshold on P_1 will set at such a level that it will remove non-bright clouds – termed cirrus quality flag.
- (iii) FAPAR is reasonably robust to the presence of cirrus clouds, while OTCI is more sensitive (see Section 4.2). Therefore, P_1 is made available to the OTCI branch as the cirrus quality flag (raised in line with MEGS8.0).
- (iv) The **OLCI** snow index (see Section 3.2) is used to identify snow and ice over land and hence reclassify the pixels. The MERIS sand flag is used to reclassify a pixel as land when identified as such.
- (v) Therefore, pixels will be classified as cloud or clear-sky land with the latter having sub-classes including ice/snow, sand and cirrus.

The classification over water of **OLCI** will be mostly based on the use of the TOA reflectance OA17 at 865 nm with the following steps:

- (i) The high bright flag is raised if rho_TOA_B16 is above a threshold; to eliminate bright clouds, high glint and sea ice. This threshold can be set to a fixed value - 0.4 is a candidate.
- (ii) The sunglint reflectance is calculated according to the Cox and Munk model and used to distinguish sunglint from cloud. Later in the processing, the sunglint module [ATBD SD-03-C09] will perform the correction in low and medium sunglint conditions and set sunglint quality flags.
- (iii) The **OLCI** snow index will be used to identify sea ice from sunglint and cloud.
- (iv) P_{scat} is calculated and used to set a cirrus cloud flag (in agreement with MEGS8.0).
- (v) A Case 2 waters flag is raised based on the rho_TOA_B16 threshold (corresponds to the maximum of the water reflectance as defined in the BWAC algorithm combined with the most turbid atmosphere tolerated by the atmospheric correction). It's a quality flag that indicates bright water pixels; a refinement will occur at the start of the BWAC module, where pixels that undergo the BWAC will be identified.
- (vi) A Case 1 flag is raised based on the rho_TOA_B16 threshold (corresponds to the most turbid atmosphere, AOT₈₆₅=0.8). It's a quality flag that indicates where the atmospheric correction may experience high aerosol loading.
- (vii) A dark quality flag has been introduced (Section 3.1), which corresponds to a quasi molecular atmosphere for which an aerosol type cannot be identified. The aerosol reflectance is obtained after subtracting the Rayleigh contribution, but could also correspond to cloud shadow.
- (viii) Therefore, pixels will be classified as cloud or clear-sky water with the latter having sub-classes including glint and sea ice that are not processed. Quality flags will be set for Case 1, Case 2, dark pixels and cirrus cloud that can be utilised within further processing modules.

Table of Contents

1.	INTRODUCTION	11
1.1	Acronyms and Abbreviations	11
1.1	Scope and Objectives	12
1.2	Algorithm Identification	13
2.	ALGORITHM DESCRIPTION: The MERIS Like Clear Sky Classification	13
2.1	The MERIS classification above Land	13
2.2	The MERIS classification above water	16
3.	APLLICATION OF A MERIS LIKE ALGORITHM FOR OLCI	20
3.1	The OLCI classification	22
3.2	The OLCI classification over land	23
3.1	The OLCI classification over water	24
4.	ALGORITHM VALIDATION	31
4.1	Evaluation of the MERIS flags	32
4.2	MERIS: flags and level 2 geophysical products	46
4.3	Summary of the MERIS Validation and Comment Relevant to the OLCI prototype	58
5.	PRACTICAL CONSIDERATION	59
6.	FUTURE EVOLUTIONS	60
6.1	Future Evolutions of the MERIS flags	60
6.2	Quality flags (indices) for the atmosphere	65
7.	ASSUMPTIONS AND LIMITATIONS including ERROR BUDGET	67
7.1	Reconsidering the role of the flags	67
7.2	Binary flag or geophysical information	67
8.	INPUT DATA	68
9.	REFERENCES	69

List of Figures

Figure 1: MERIS classification over land	14
Figure 2: (a) Examples of spectra for coarse and fine grain snow (snow1 and snow 2) and (b) Impact of the Rayleigh reflectance on ratio 443 nm / 750 nm and hence spectral test for sand. 16	
Figure 3: MERIS classification over water	17
Figure 4: MERIS land-water radiometric reclassification in the absence of sunglint.....	19
Figure 5: OLCI scanning mode.....	21
Figure 6: General OLCI classification flow chart.....	23
Figure 7: Land Decision Flags – binary (Baseline).....	24
Figure 8: Water Decision Flags – binary (Baseline).....	25
Figure 9: RGB MERIS image in the Arctic Ocean offshore of Siberia, 27 May 2003, centre of image: 132.09E 83.03N.....	26
Figure 10: RGB MERIS image offshore of Greenland, 27 May 2003, centre of image: 132.09E 83.03N.....	26
Figure 11: MERIS spectral TOA reflectance for different ice situations.....	27
Figure 12: MNSI over the Arctic Ocean; values are above the 0.01 threshold.....	27
Figure 13: MNSI over the Arctic Ocean above the 0.01 threshold.....	28
Figure 14: RGB MERIS in the mouth of the Amazon River, 27 May 2003, centre of image: 132.09E 83.03N.....	30
Figure 15: On the Amazon transect, B13 TOA reflectance (blue diamonds) and level 2 SM (pink squares).....	31
Figure 16: RGB MERIS image, France, 09 September 2004.....	32
Figure 17: Level 2 reflectance in channel B2 over France, 09 September 2004. Region of Interest used is indicated by the red rectangle.....	33
Figure 18: Frequency in L2 reflectance channel B2 within the Region of Interest.....	33

Figure 19: 09 March 2007 MERIS image showing pins for fresh snow and melting snow. The TOA reflectance for the pin locations, fresh snow (violet squares) and melting snow (blue diamonds), plus a typical cloud (orange diamonds).....34

Figure 20: MERIS images showing pins at (a) 12 April 2005 White Sands at 106.20W 32.99N and (b) Libyan desert, 11 January 2005 at 22.5E 26.36N. (c) The TOA reflectance for the pin locations; sand in Libya (blue diamonds), white sand (yellow triangles) and cloud (red squares).
.....36

Figure 21: (a) RGB MERIS image of a dust episode, Atlantic Ocean, 06 March 2004. (b) Plot of B13 TOA reflectance and level 2 flags: Cloud flag (pink squares), PCD_13 flag (yellow triangles) and PCD_15 flag (cyan squares).....39

Figure 22: (a) RGB MERIS image of a dust area over Saharan outbreak, 04 November 2003. (b) TOA reflectance (pink squares) scaled on the left axis with Absoa_dust (cyan squares), PCD_13 flag (blue diamonds) and PCD_15 flag (yellow diamonds) appearing only when the flag is raised.....40

Figure 23: (a) RGB MERIS image of the English Channel, 09 September 2004. (b) TOA reflectance (pink squares) scaled on the left axis with Absoa_dust (violet crosses), PCD_13 flag (yellow diamonds) and PCD_15 flag (cyan crosses) appearing only when the flag is raised.41

Figure 24: (a): RGB MERIS image of a glint area in the Pacific Ocean, day 2005/05/20, and centre of picture: long: -143.33, lat: 30.11. (b): TOA reflectance (blue cross) scaled on the left along the transect GCP2 to GCP3. Medium glint (pink square) and high glint (yellow diamond) appear when the flag is raised.43

Figure 25: (a) RGB MERIS, Pacific Ocean, day 2005/05/17, long: -144.01W, lat: 22.42N (b) TOA B13 reflectance (blue diamond). And flags: Medium glint (cyan cross), high glint (yellow diamond) and cloud flag (pink point)44

Figure 26: MERIS RGB for (a) Spain on 04 June 2004, (b) English Channel on 09 September 2004, (c) Amazonia on 04 June 2004 and (d) Gulf of Mexico on 04 April 2005. Plots along the transects of (e) Ratio TOA_B13/TOA_B8 with (a) blue diamonds, (b) pink squares, (c) yellow triangles and (d) green crosses for each date.45

Figure 27: MERIS images over the Britain and France (1.26W 47.85N).46

Figure 28: MERIS L2 product along the transect: (a) BRR_B2 and PCD_, (b) AOT_B2, (c) MGVI, (d) MTCI.....47

Figure 29: English Channel transect: (a) AOT at 865 nm; (b) Angstroem coefficient; (c) different PCDs: PCD_13=1, PCD_15=0.9, PCD_16=0.8, PCD_17=0.7, PCD_19=0.9;(d) Chlorophyll a content for case 1 algorithm (blue diamonds) and case 2 algorithm (pink squares);(e) yellow substance and (f) total suspended matter.....49

Figure 30: Transects for MERIS Atlantic Ocean image from 06 April 2004 showing (a) flags; (b)AOT_865 nm; (c) Angstroem coefficient; (d) alga_1 (blue diamond) and alga_2(yellow triangle) in µg/l.50

Figure 31: TOA reflectance along the transect at different distances.51

Figure 32: Saharan outbreak on 04 November 2003 with a transect showing (a) flags, (b) AOT and (c) Angstroem coefficient.52

Figure 33: MERIS image over the Pacific Ocean on 20 May 2005 with transects of B13 TOA reflectance and aerosol product (AOT_865 and Angstroem coefficient) plotted.....54

Figure 34: MERIS image over the Pacific Ocean on 20 May 2005 with transects for the TOA_reflectance (violet square) and level 2 products plotted.56

Figure 35: RGB MERIS images over Atlantic Ocean, centre of images are 42.49W 27.80N.....56

Figure 36: (a) Flags, (b) AOT and (c) chlorophyll a for the MERIS image over Atlantic Ocean..57

Figure 37: (a) RGB MERIS image from 09 March 2007 and (b) resulting MNSI.61

Figure 38: Apparent pressure (P1) plotted against AOT at 443 nm for MERIS transect across French Brittany on 09 September 2004.62

Figure 39: Apparent scatter pressure (P_{scat}) versus AOT at 865 nm plotted for a MERIS transect across the British Channel on 09 September 2004.63

Figure 40: Sunlint over the Atlantic Ocean on 07 June 2004 with (a) L2 cloud mask shown and (b) O2 derived pressure plotted along a transect.....64

Figure 41: (left) RGB MERIS image over the Portugal Coast: (12.94W 43.37N) on 07 September 2006. (right) B13 TOA reflectance and L2 flags (CLOUD) along the transect.....66

List of Tables

Table 1: MERIS level 1 flags.....	13
Table 2: OLCI versus MERIS spectral bands	21
Table 3: MERIS spectral ratios for melting snow, fresh snow and cloud	35
Table 4: MERIS spectral ratio for two types of sand and a cloud	35
Table 5: Definition of MERIS PCDs over water	37
Table 6: Chlorophyll and aerosol products in the vicinity of a cloud.	66

1. INTRODUCTION

1.1 Acronyms and Abbreviations

AATSR	Advanced Along Track Scanning Radiometer
ABSOA	L2 MERIS flag: ABSorption Of Aerosol
AERONET	AERosol ROBotic NETwork
AOT	Aerosol Optical Thickness
ATBD	Algorithm Theoretical Basis Document
AVHRR	Advanced Very High Resolution Radiometer
BEAM	Basic ERS and Envisat (A)ATSR and MERIS Toolbox
BPAC	Bright Pixel Atmospheric Correction
BRR	Bottom of Rayleigh Reflectance
DEM	Digital Elevation Map
DPM	Detailed Processing Model
EC	European Commission
ESA	European Space Agency
FR	Full Resolution
GMES	Global Monitoring of Environment and Security
ICOL	Improve Contrast between Ocean and Land
IOP	Inherent Optical Properties
LUT	Look-Up Table
MDSI	MERIS Differential Snow Index
MERIS	MEDium Resolution Imaging Spectrometer (http://envisat.esa.int/instruments/MERIS/)
MGVI	MERIS Global Vegetation Index
MNSI	MERIS Normalised Snow Index
MODIS	MODerate resolution Imaging Spectroradiometer
MTCI	MERIS Terrestrial Chlorophyll Index
NDSI	Normalised Differential Snow Index
NIR	Near Infra Red
PAR	Photosynthetically Available Radiation
OLCI	Ocean Land Colour Instrument
RGB	Red Green Blue
ROI	Region Of Interest
RR	Reduced Resolution
RTC	Radiative Transfer Code
S3	Sentinel 3
SLSTR	Sea and Land Surface Temperature Radiometer
SAM	Standard Aerosol Mode
SeaWiFS	Sea-viewing Wide Field-of-view Sensor
SOS	Successive Orders of Scattering code

<p>Richard <i>SANTER</i> (LISE)</p> 	<p>SENTINEL-3 OPTICAL PRODUCTS AND ALGORITHM DEFINITION</p> <p>OLCI Level 2 Algorithm Theoretical Basis Document Pixel Classification</p>	<p>Ref: S3-L2-SD-03-C01-LISE-ATBD Issue: 2.3 Date: 17/07/10 Page 12 of 69</p>
--	--	---

TOA Top Of Atmosphere
ULCO Université du Littoral Côte d'Opale (Wimereux – France)
 (<http://www.univ-littoral.fr>)

1.1 Scope and Objectives

The aim of the classification is to distinguish water and land i.e. it will be designed to separate pixels into the water and land chains as there is currently no OLCI atmospheric processing chain. This is also the case for SeaWiFS over the ocean where the bright pixel flag deactivates the ocean colour branch. So, for example, there is no *a priori* need to identify a cloud if the presence of a cloud is already rejected by the flag(s) used in the decision matrix; a classical cloud screening is not required and a clear sky flag can be only evaluated through the level 2 products and not through a classical “meteorological” assessment of cloud occurrence. This understanding will also drive the validation of the flags.

Following the spirit of MERIS, in terms of level 2 products and associated algorithms, the needs (in terms of classification) are identified in terms of what is re-usable from MERIS and then the document lists the limitations.

1.2 Algorithm Identification

This algorithm is identified under reference “SD-03-C01” in the Sentinel-3 OLCI documentation.

2. ALGORITHM DESCRIPTION: The MERIS Like Clear Sky Classification.

Table 1 lists the MERIS level 1 flags, which will be referred to in the following sections.

Table 1: MERIS level 1 flags

COSMETIC	1	Pixel is cosmetic
DUPLICATED	2	Pixel has been duplicated (filled in)
GLINT_RISK	4	Pixel has glint risk
SUSPECT	8	Pixel is suspect
LAND_OCEAN	16	Pixel is over land, not ocean
BRIGHT	32	Pixel is bright
COASTLINE	64	Pixel is part of a coastline
INVALID	128	Pixel is invalid

2.1 The MERIS classification above Land

First, the TOA radiances are converted into Top of Atmosphere (TOA) reflectances and then the gaseous absorption correction is applied. For the selected MERIS bands (B2, B10 and B12), the classification is applied on the Bottom of Rayleigh Reflectance (BRR). The Rayleigh correction is applied because of the large variation in the surface pressure due to the elevation of the site.

Figure 1 is a paste and copy of the MERIS Detailed Processing Model (DPM) (Bourg et al., 2009). The basic test is the bright pixel flag in the blue part of the electromagnetic spectrum. Use of the O₂ pressures (surface and cloud top) was initially implemented, but not activated because of the poor quality of the O₂ pressure estimates. However, this has been included in

the latest version of the DPM (Bourg et al., 2009) as it is being included in the 2010 MERIS reprocessing; it is also described in Santer and Brockmann (In Press). When the O₂ pressures are used, additional tests are based on the comparison between the O₂ derived pressures and the barometric pressure at the surface obtained from the sea level meteorological pressure and the Digital Elevation Model (DEM) to reduce the pressure exponentially with the site elevation; the B2 radiometric test and O₂ test are included in the decision matrix.

The bright land pixels are primary clouds, but it they can also be sand or snow. Therefore, the bright land pixels are examined to identify snow or sand. If this is the case then these pixels are fed back into the land processor. Figure 1 is a schematic showing this decision process.

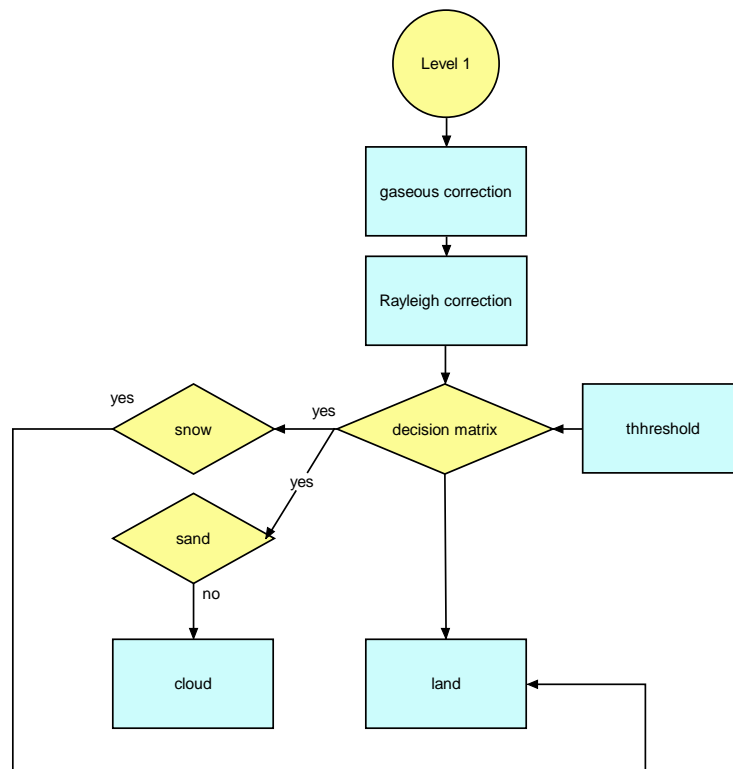


Figure 1: MERIS classification over land

a) **The bright pixel flag:** The land surface (except snow and sand) is relatively dark in the blue part of the electromagnetic and the Rayleigh contribution is known. The maxima of the surface reflectance and aerosol loading are defined; this flag can also accept aerosol turbidity up to a

certain level. If the aerosol loading is too high, it's assumed that it's not possible to process the land algorithm first the aerosol remote sensing module and second the surface characterization.

b) **Setting the land decision matrix threshold:** The Rayleigh corrected reflectance at 442.5 nm is compared with radiometric thresholds ρ_{rc_LUT} . If the BRR is lower than the threshold, the pixel is considered as a non bright pixel. Else, it is a bright pixel. The threshold is computed (Zagolski et al., 2005) as a function of the solar zenith angle, satellite zenith angle and relative azimuth angle between sun and viewing directions. Initially, the SOS code (Deuzé et al., 1989) is run with the following inputs:

- Surface pressure of 1013 hPa.
- Lambertian surface of reflectance $\rho_s=0.1$.
- Aerosol optical thickness (AOT) at 550 nm equal to 2.
- Continental aerosol model.

A second SOS run is done for a pure molecular atmosphere over a dark target. The difference between the two runs, which corresponds to a Rayleigh corrected TOA reflectance, is used to set the threshold. The atmospheric inputs to the threshold are controlled by the limits of the aerosol remote sensing module; the limit to $\rho_s=0.1$ is an initial guess.

c) **Snow:** The reflectance of the snow significantly decreases the reflectance in the Near Infra-Red (NIR) as illustrated in [Figure 2a](#); more significant than for the clouds. When the initial MERIS classification ATBD was produced (1997) the dynamic range of B13 was such that the signal above snow could saturate and the spectral position of B14 (between 885 nm and 890 nm) was not finalised. Therefore, B12 (778 nm) was selected as the NIR band and B10 (751 nm) as the visible band. So, the classification test was applied to the TOA B10/B12 reflectance ratio after correction for the gaseous absorption and Rayleigh scattering. The threshold was set empirically.

d) **Sand:** Sand is yellow with its reflectance significantly decreasing in the blue part of the electromagnetic spectrum. Therefore, the classification test applies to the ratio B2/B10 and using B2 over land requires a Rayleigh correction. [Figure 2b](#) is the sensitivity of the ratio to the surface pressure which justifies the Rayleigh correction.

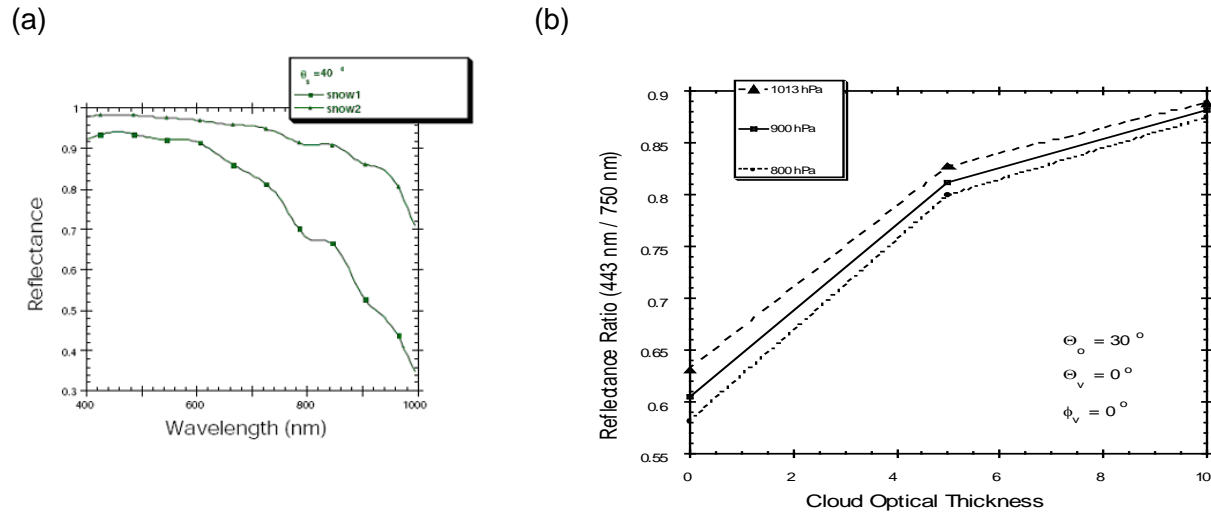


Figure 2: (a) Examples of spectra for coarse and fine grain snow (snow1 and snow 2) and (b) Impact of the Rayleigh reflectance on ratio 443 nm / 750 nm and hence spectral test for sand.

2.2 The MERIS classification above water

Figure 3 is a paste and copy from the MERIS DPM. The water classification is based on the TOA reflectance after correction for the gaseous absorption and Rayleigh scattering. Outside the sunglint, a bright pixel flag discriminates cloud from water. Above sunglint, a high glint flag is applied to prevent the water processing, but to allow the retrieval of water vapour. The outputs also include a set of quality flags.

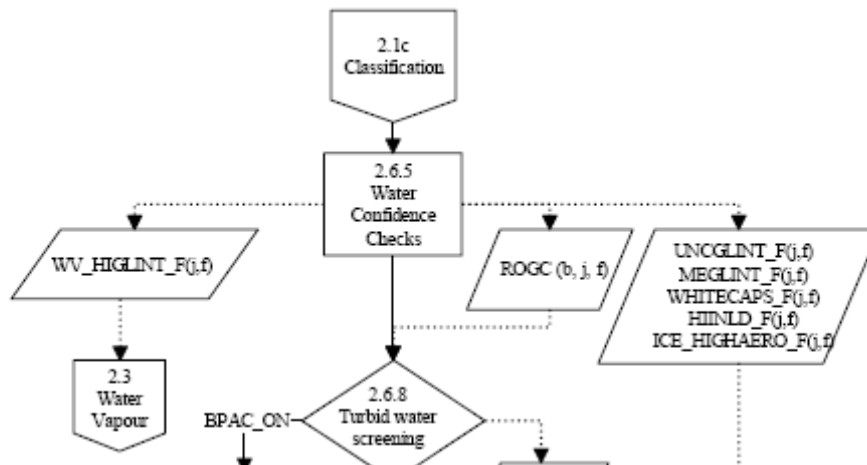


Figure 3: MERIS classification over water (truncated as the original diagram includes more than classification).

a) **Bright pixel:**

This is a similar approach to that applied over land using B2. The water surface is quite dark. The Rayleigh contribution can be calculated and the approach can accept aerosol turbidity up to a certain level; the maxima of the surface reflectance and aerosol loading are defined. If the aerosol loading is too high, it's assumed that it's not possible to progress with the water processing branch.

The Rayleigh corrected reflectance at 442.5 nm is compared with radiometric thresholds Rho_{rc_LUT} . If the BRR is lower than the threshold, the pixel is considered as a non bright pixel. Else, it is a bright pixel. The threshold is computed (Santer and Brockmann, In Press) as a function of the solar zenith angle, satellite zenith angle and relative azimuth angle between sun and viewing directions. The SOS code is first run with the following inputs, but with the direct sunglint excluded:

- Surface pressure of 1013 hPa.
- Lambertian surface of reflectance $\rho_s=0.036$.
- Aerosol optical thickness (AOT) at 550 nm equal to 2.
- Maritime aerosol model.

A second SOS run is undertaken for a pure molecular atmosphere over a dark target. The difference between the two runs, which corresponds to a Rayleigh corrected TOA reflectance, is used to set the threshold.

b) **Sunglint flags:** High and medium glint flags are set on radiometric basis (Montagner et al., 2003).

c) **Reclassification in absence of sunglint:** The level 1 MERIS product has two geographically based flags to distinguish land from water: the land-ocean and the coastal flags. For the ocean, there are several limitations to these flags:

- i. Error within the flags.
- ii. Error in the MERIS geo-localisation.
- iii. Temporal variation of the coastline (tide, erosion etc).

Therefore, ESA decided to apply a radiometric consolidation of the land-ocean classification. During the first MERIS processing, it only applied to pixels near the coastline. Then, to fulfil the requirements of the inland water community (artificial reservoirs were not identified through the geographic flags), it was decided to extend this radiometric reclassification over land.

First, in the red and NIR, the water is relatively dark compared to the land. Therefore, an initial test is used to eliminate the bright land pixels – based on the BBR test. The contrast is greater in the NIR than the red, but the adjacency effect reduces the contrast and varies strongly with the distance of the pixels from the land (or from the water if we're above land) and so it's difficult to propose a threshold. So, although the land-water contrast is lower in the red which reduces the adjacency effect, it is significant enough to exclude too bright land pixels and is the basis of the first test.

Between the red and NIR, the BRR above water decreases. Conversely, the BRR increases over land. Therefore, the second test is based on the ratio of the BRR between B8 (665 nm) and B13 (865 nm). **Figure 4** summarises these two tests within a flow diagram.

The first threshold is set similarly to the bright pixel threshold; based on the use of Radiative Transfer Code (RTC) with a turbid maritime aerosol over dark water. The second threshold is set empirically.

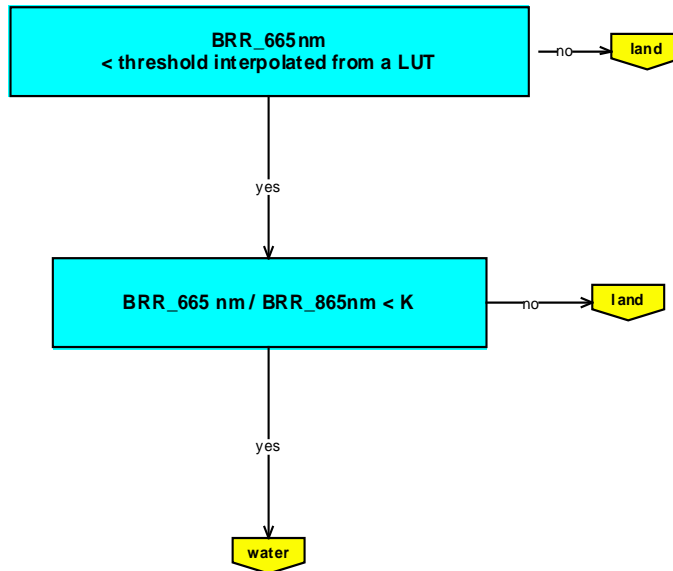


Figure 4: MERIS land-water radiometric reclassification in the absence of sunglint.

d) **Reclassification in presence of sunglint:** In presence of sunglint, the reclassification based on the absence of sunglint is no longer valid. The Fresnel reflection is white but, because of the stronger atmospheric attenuation at 665 nm than at 865 nm, the apparent contribution of the sunglint is higher at 865 nm than at 665 nm. If the sunglint becomes too high, it's no longer possible to use the radiometric measurements of a signal pixel in order to distinguish between a cloud and sunglint. In such cases it's better to test for high sunglint (uses L1b land-water flag, geometry and wind) and keep the L1b classification instead of switching to a radiometric test.

3. APPLICATION OF A MERIS LIKE ALGORITHM FOR OLCI

Table 2 shows the correspondence in spectral bands between OLCI and MERIS. For pixel classification in MERIS we needed:

- i. 443 nm over land because it's dark.
- ii. 443 nm over water was used in MERIS to be in line with the classification over land. For OLCI, we proposed to use 865 nm.
- iii. 412/753 for a slope test on sand.
- iv. 753/865 for a slope test on sand.
- v. 665/865 for a slope test on water.
- vi. 761/753 for the O₂ transmittance and derived pressures. The additional O₂ OLCI band is a potentiality for a better classification
- vii. The MERIS snow index between 865-885 is replaced in OLCI by 865-1020.

Also, for OLCI compared to MERIS, the whole field-of-view is shifted across-track by 12.2 degrees away from the sun to minimise the sun-glint impact (see Figure 5). The impact is not on the classification method, but in the definition of the threshold Look-Up Tables (LUTs).

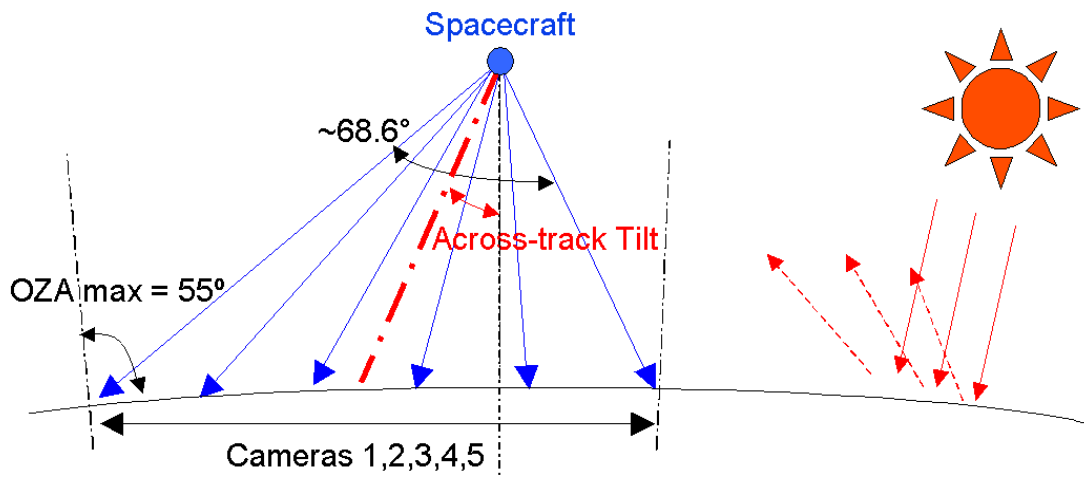


Figure 5: OLCI scanning mode.

Table 2: OLCI versus MERIS spectral bands

OLCI band	central wavelength	spectral width	MERIS band	central wavelength	spectral width
O1	400	15			
O2	412.5	10	01	412.5	10
O3	442.5	10	02	442.5	10
O4	490	10	03	490	10
O5	510	10	04	510	10
O6	560	10	05	560	10
O7	620	10	06	620	10
O8	665	10	07	665	10
O9	673.75	7.5			
O10	681.25	7.5	08	681.25	7.5
O11	708.75	10	09	708.75	10
O12	753.75	7.5	10	753.75	
O13	761.25	2.5	11	761.75	3.75
O14	764.375	3.75			
O15	767.5	2.5			
O16	778.75	15	12	778	15
O17	865	20	13	865	15
O18	885	10		885	10
O19	900	10		900	10

O20	940	20			
O21	1020	40			

The **OLCI** and MERIS levels 1 are radiances. The classification will not apply on the level 1 TOA radiance but on the TOA reflectance.

The useful geographical level 1 flags are based on a priori knowledge: land-ocean and coastline. A key issue is to have the best geographical references, including for inland waters. This level 1 classification between land and water is a key element.

In addition, OLCI had the 1.02 μm band. Snow & ice can be discriminated from cloud using the slope in the NIR, which the band at 1.02 nm (if not saturated) can aid with. There is also an additional oxygen band that may help to refine the determination of the O₂ pressures with positive impact on the classification.

3.1 The **OLCI** classification

Figure 6 shows the overall schematic for the classification process. What we expect from the level 1 flags are:

- Bright flag over ocean identifies bright cloud, sea ice and high glint.
- Land_water flag over the ocean identifies the coastal areas for which a radiometric reclassification of water and land is needed.
- Glint risk flag activates the level 2 sun glint flags.

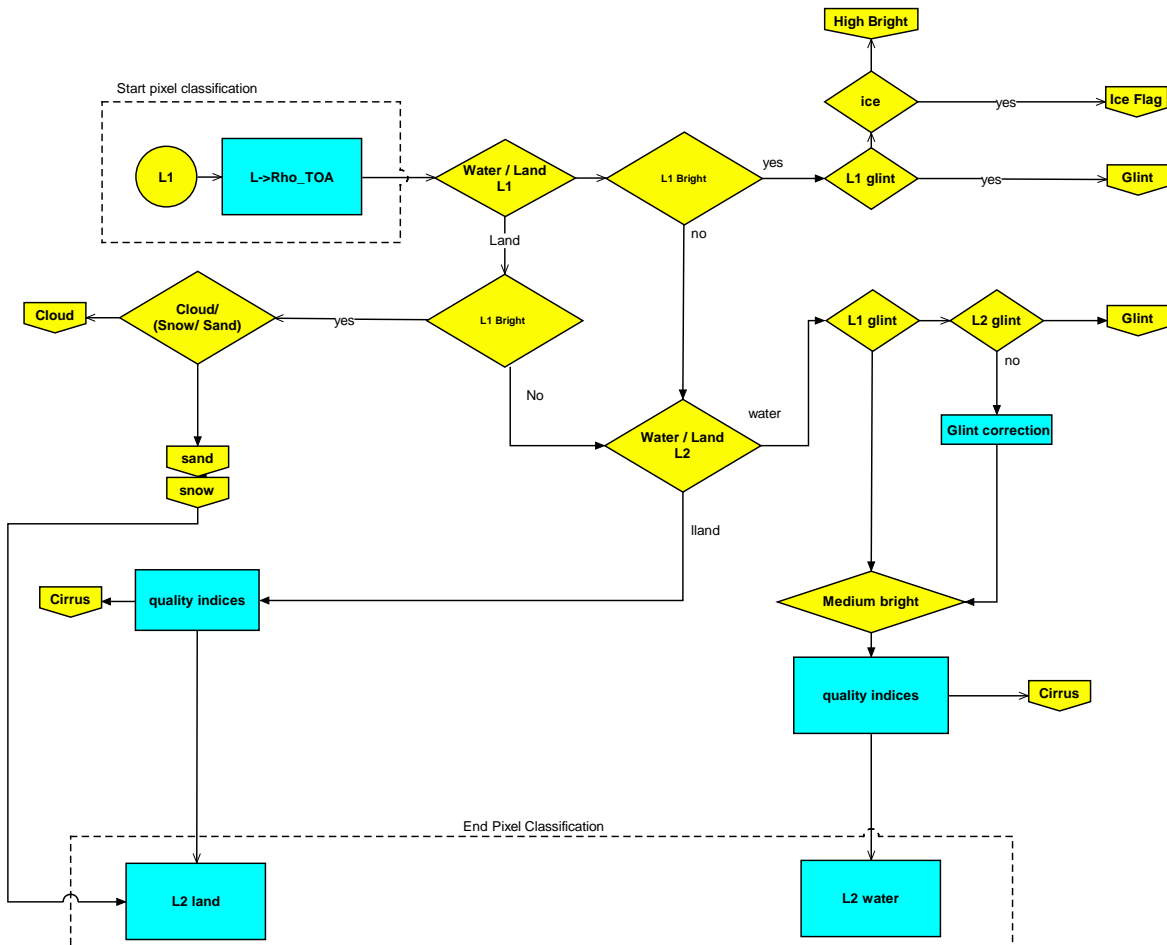


Figure 6: General OLCI classification flow chart.

3.2 The OLCI classification over land

The water decision flags are shown as a schematic in Figure 7. The level 1 bright flag over land is first used to identify bright cloud, ice/snow and sand. If the L1 bright flag is raised then the pixel goes first to the snow and second to the sand tests. If either is positive then corresponding flag is raised and the pixel goes directly go to the land processing branch. The ONSI will be used for snow identification and sand identification is identical to that used for MERIS, but it can be conducted without gaseous and Rayleigh correction.

When the L1 bright flag is not raised, then the pixel goes to the L2 land_water radiometric classification. If land is confirmed, the required land quality “atmospheric” indices (and output these indices) are set and the pixel goes to the land processing branch.

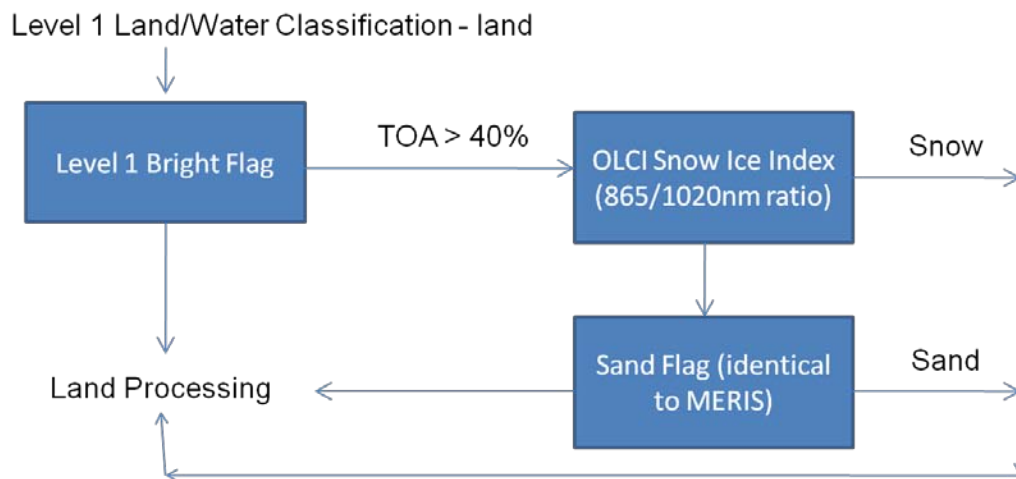


Figure 7: Land Decision Flags – binary (Baseline).

3.1 The **OLCI** classification over water

The water decision flags are shown as a schematic in **Figure 8** and the summary is:

- The L1 land/water pixel goes to water.
- If the L1 bright is raised the pixel will not process except for ice identification, which is conducted if the L1 sunglint risk is not raised. If the L1 bright is not raised, it's confirmed that we are above water.
- If there is a risk of sunglint and the sunglint correction is not possible then the L2 glint flag is raised. If it's possible the sunglint correction is applied at least at 865 nm.
- The medium bright L2 test is applied to indicate if the atmospheric correction is feasible. If yes, the quality indices are computed and the pixel proceeds to the ocean processing branch.

NB: The second medium L2 test can be applied after the atmospheric correction.

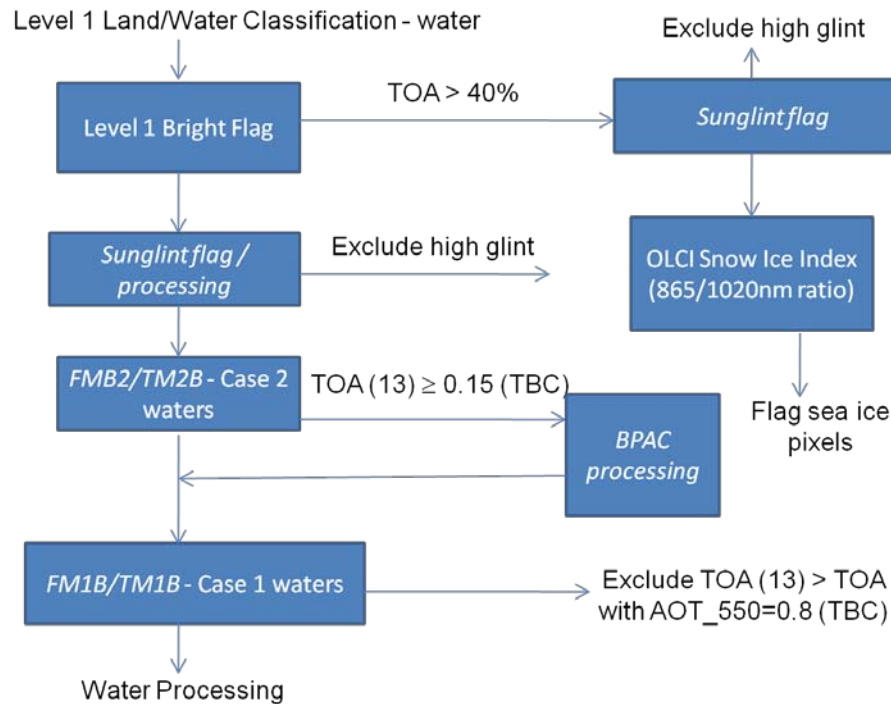


Figure 8: Water Decision Flags – binary (Baseline).

Flagging of the sea ice (the sea ice flag, FSI)

It's assumed there is sun glint contamination when the algorithm is looking for sea ice. When the level 1 cloud flag is raised it could be identifying sea ice. The differentiation between ice and clouds is visual, and an example over the Arctic Ocean is shown in Figure 9; when looking at the RGB image the interpretation is that it's ice or breaking ice (presence of water). A second example is provided for Greenland; Figure 10.

The spectral signatures of the TOA reflectance above ice are shown in Figure 11; the small gap between B4 and B7 corresponds to the oxygen absorption. For sea ice the TOA reflectance decreases between B13 and B14, which supports the use of the MNSI for ice identification. This MNSI is applied to an image including Siberian Arctic ice, see Figure 12. The threshold was set as 0.01 and the ice flag would be appropriately raised as all pixels are above this value.



Figure 9: RGB MERIS image in the Arctic Ocean offshore of Siberia, 27 May 2003, centre of image: 132.09E 83.03N.



Figure 10: RGB MERIS image offshore of Greenland, 27 May 2003, centre of image: 132.09E 83.03N.

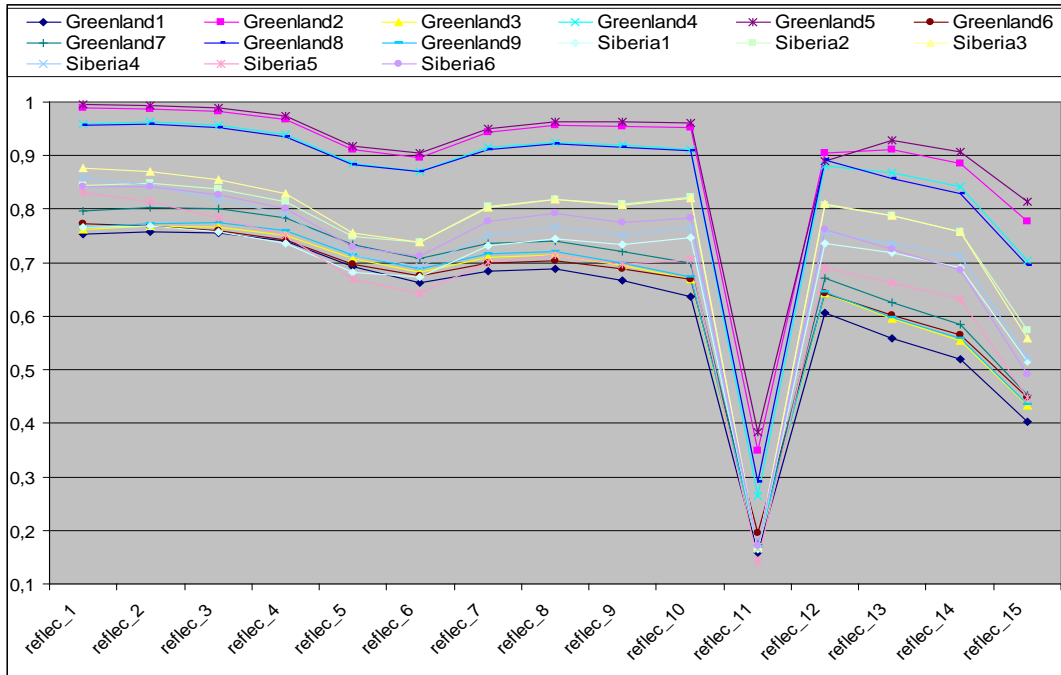


Figure 11: MERIS spectral TOA reflectance for different ice situations.

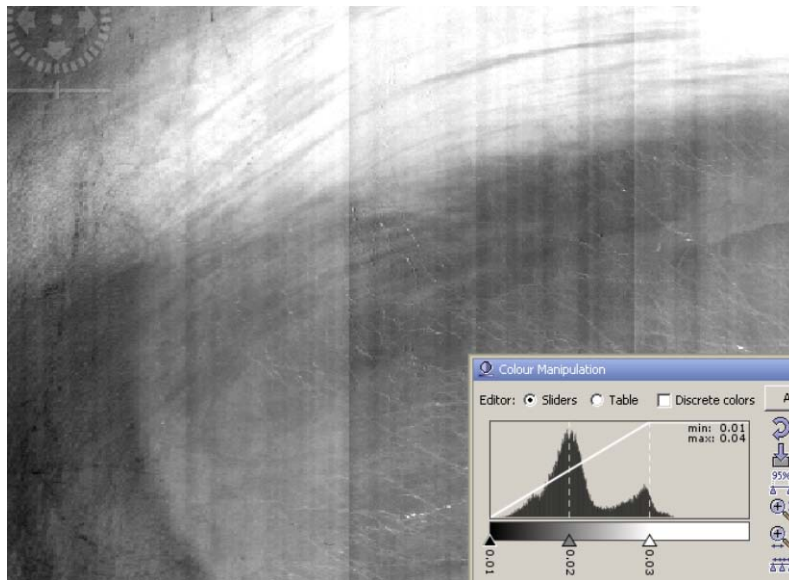


Figure 12: MNSI over the Arctic Ocean; values are above the 0.01 threshold.

The MNSI, with the same threshold, was also successfully applied to a Greenland scene, see **Figure 13**. On the right of the image the situation appears confused, but the RGB image clearly shows floating ice.

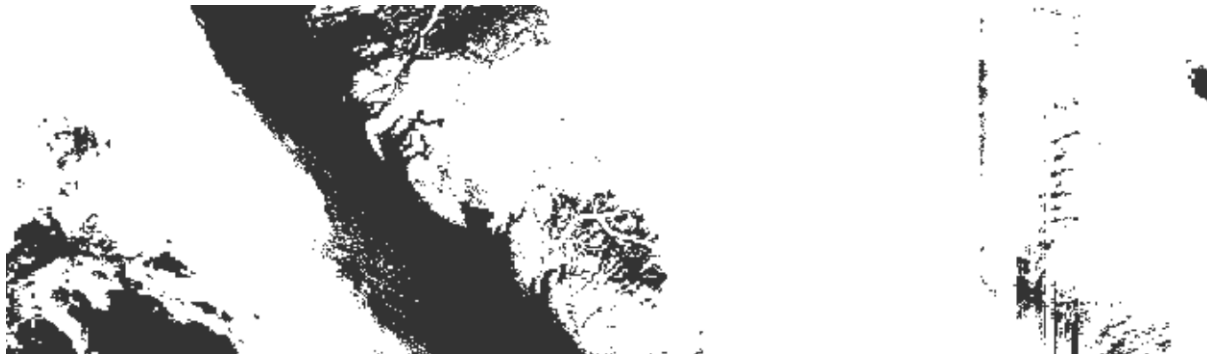


Figure 13: MNSI over the Arctic Ocean above the 0.01 threshold.

The additional of the OLCI band at 1.02 μm allows the introduction of an **OLCI** snow index, which improves sea ice detection (Stamnes et al., 2007):

$$ODSI = \frac{rho_{toa}(865) - rho_{toa}(1020)}{rho_{toa}(865) + rho_{toa}(1020)}$$

The sea ice flag doesn't impact the water processing chain; it just flags the pixels as sea ice rather than cloud.

The sunglint flag

It's inconsistent to apply a sunglint correction in the medium glint area and not in the high sunglint area if the ocean processing is applied as the role of the sunglint flag should be to indicate when a sunglint correction is applicable. Above, the ocean processor is not activated.

The level 2 medium bright flags (FM1B & FM2B)

The objective of FM1B and FM2B are to decide whether to go (or not) into the water processing branch; it replaces the MERIS level 2 bright pixel flag. The first element of the water processing is the aerosol model retrieval, which is conducted (for MERIS) using B12 and B13 with the input being the TOA reflectance corrected for gaseous absorption and sunglint. In B12 and B13, the gaseous absorption is residual and therefore do not need to be done.

Compares to MERIS, it's proposed to use B13 instead of B2. In B13, for the open ocean, the small variations of the barometric pressure will have a residual impact on the setting of the threshold. Over inland water, the threshold will be set higher than it should be because of the reduced Rayleigh contribution in the satellite signal. More pixels over land will "wrongly" go in the water box, but they will be flagged later. The FMB requires neither a gaseous correction nor a Rayleigh correction.

The sunglint correction is applied when the level 1 glint risk is raised. The regular sunglint correction refers to the Cox and Munk (R8) model and uses the wind speed as input. The atmospheric attenuation is applied for a pure molecular atmosphere. The aerosol extinction is ignored. B13 is more favourable because it is expected that this extinction is less effective than in B2.

Threshold for case 1 water, TM1B

As water is black, the aerosol remote sensing applies up to an Aerosol Optical Thickness (AOT) at 550 nm of 0.8 for n standard aerosol models (SAMs). The B13 TOA reflectance is generated as follows:

- Standard barometric pressure of 1013 hPa.
- No direct sunglint.
- Standard wind speed of 7.2 m/s.
- Geometrical grid of MERIS LUT.
- $AOT_{550}=0.8$ (TBC).
- An iterative loop on the SAMs.

At the end, for each geometry, the threshold is set to the maximum value among the n SAMs. Alternatively, the atmospheric correction LUTs (ATBD SD-03-C07) can be used to generate the thresholds.

Threshold for case 2 water, TM2B

Over case 2 waters, the contribution of the water body to the TOA reflectance should be taken into account. As an extreme for the turbid water a MERIS image collected over the mouth of the Amazon River was selected, see [Figure 14](#), with a transect crossing the sediment plume. For this transect, the B13 TOA reflectance (left axis) and the level 2 Suspended Matter (SM) (right scale, mg/l) are shown versus the pixel number from P1 to P2; see [Figure 15](#). The SM is set to zero when the cloud flag is raised. The performance of the BPAC (Moore and Lavender, 2010) is limited to a maximum SM value of 50 mg/l although it can be slightly above. Around 50 mg/l, the TOA reflectance in B13 is 0.15, which is a good basis for setting *TM2B*.

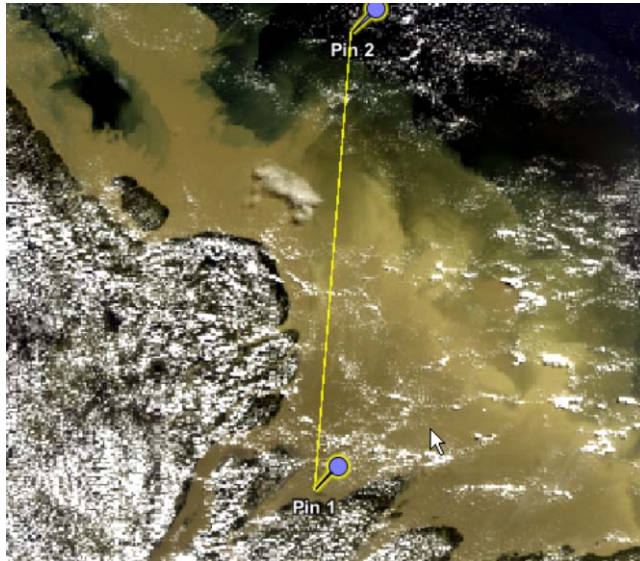
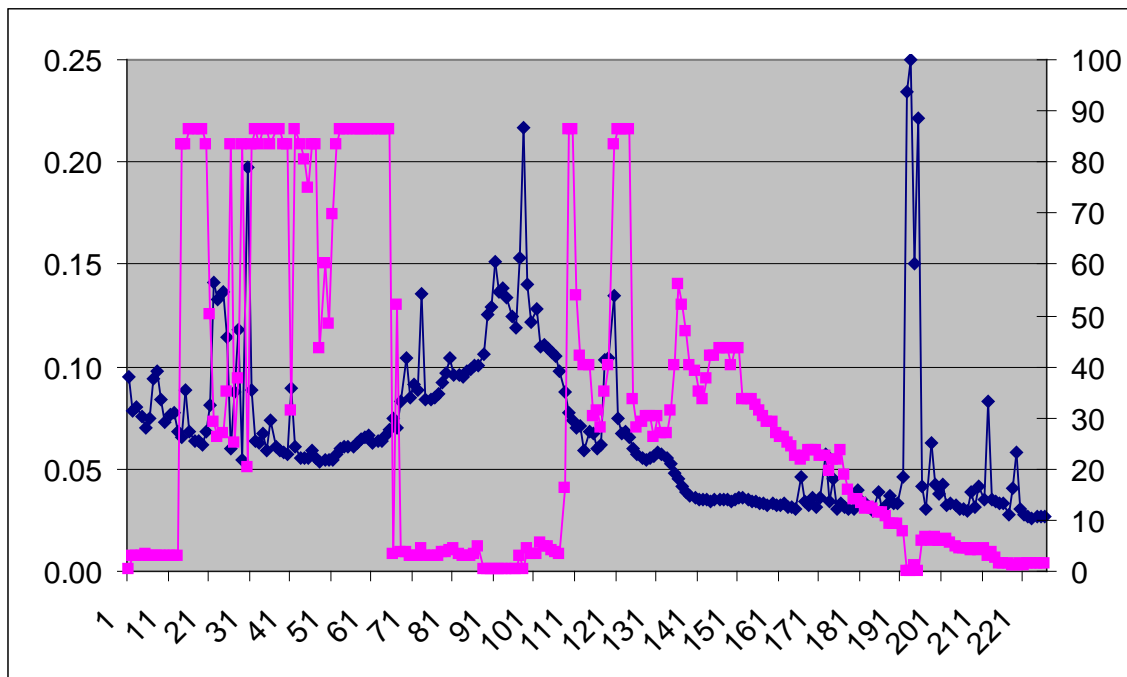


Figure 14: RGB MERIS in the mouth of the Amazon River, 27 May 2003, centre of image:
132.09E 83.03N.



<p>Richard <i>SANTER</i> (LISE)</p> 	<p>SENTINEL-3 OPTICAL PRODUCTS AND ALGORITHM DEFINITION</p> <p>OLCI Level 2 Algorithm Theoretical Basis Document</p> <p>Pixel Classification</p>	<p>Ref: S3-L2-SD-03-C01-LISE-ATBD Issue: 2.3 Date: 17/07/10 Page 31 of 69</p>
--	---	---

Figure 15: On the Amazon transect, B13 TOA reflectance (blue diamonds) and level 2 SM (pink squares)

Combining TM2B and TM1B

The sequence is the following (also shown in [Figure 8](#)):

- i. Input the TOA_B13 reflectance.
- ii. Correct from the sunglint if the sunglint risk flag is raised.
- iii. Test with *TM2B*.
- iv. If $RO_TOA_B13 < TM2B$ then apply the BPAC.
- v. Use RO_TOA_B13 after correction of the water body contribution for the test with *TM1B*.
- vi. Go to the water processor.

FM1B and FM2B are decision flags.

The dark flag: FD

The aerosol reflectance is obtained after subtracting the Rayleigh contribution. Therefore, when the TOA reflectance is very close to the Rayleigh contribution any ratio between the aerosol reflectance at two spectral bands will be subject to a very large error. This is the case for both the selection of the aerosol model and determination of P_{scat} . Therefore, the test is based on a comparison between the B13 TOA reflectance, after sunglint correction, and the B13 Rayleigh reflectance. If $TOA_B13 > Ray_B13 * TD$, then the aerosol model is selected by default. P_{scat} is set to 1013 hPa.

NB: It may happen than this dark flag also corresponds to cloud shadow.

4. ALGORITHM VALIDATION

4.1 Evaluation of the MERIS flags

Over land

a) **Setting the land decision matrix threshold:** One MERIS image that was a clear day over France was selected; see [Figure 16](#). In the sub-setted Region of Interest (ROI), see [Figure 17](#), no cloud was detected by visual inspection. The histogram of the level 2 surface reflectance, see [Figure 18](#), indicates that the surface reflectance is below the threshold of 0.1. AERONET data (Palaiseau is in the middle of the ROI) provides an order of magnitude for the aerosol optical thickness. At the time of MERIS overpass, the AOT at 440 nm was 0.1 which corresponds to a horizontal visibility of 50 km. The MERIS surface reflectance is actually the reflectance of the surface combined with the aerosol scattering. Therefore, the surface reflectance should be shifted by approximately -0.01 and a value of 0.1 is reasonable.



Figure 16: RGB MERIS image, France, 09 September 2004



Figure 17: Level 2 reflectance in channel B2 over France, 09 September 2004. Region of Interest used is indicated by the red rectangle.

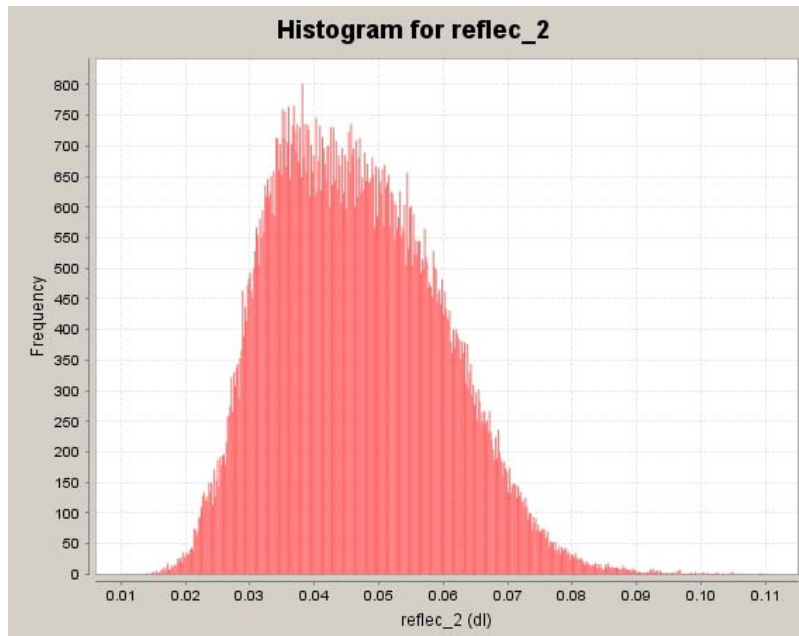


Figure 18: Frequency in L2 reflectance channel B2 within the Region of Interest.

- | b) **Snow versus cloud**: Two MERIS images over the Alps were selected; see [Figure 19 a & b](#). The cloud flag is raised over the snow and the reclassification of bright pixels into snow pixels failed. To better understand this, two pins are extracted and the TOA reflectance in all the MERIS bands shown; see [Figure 19c](#). In addition, the typical MERIS signal over a cloud is also extracted and plotted.

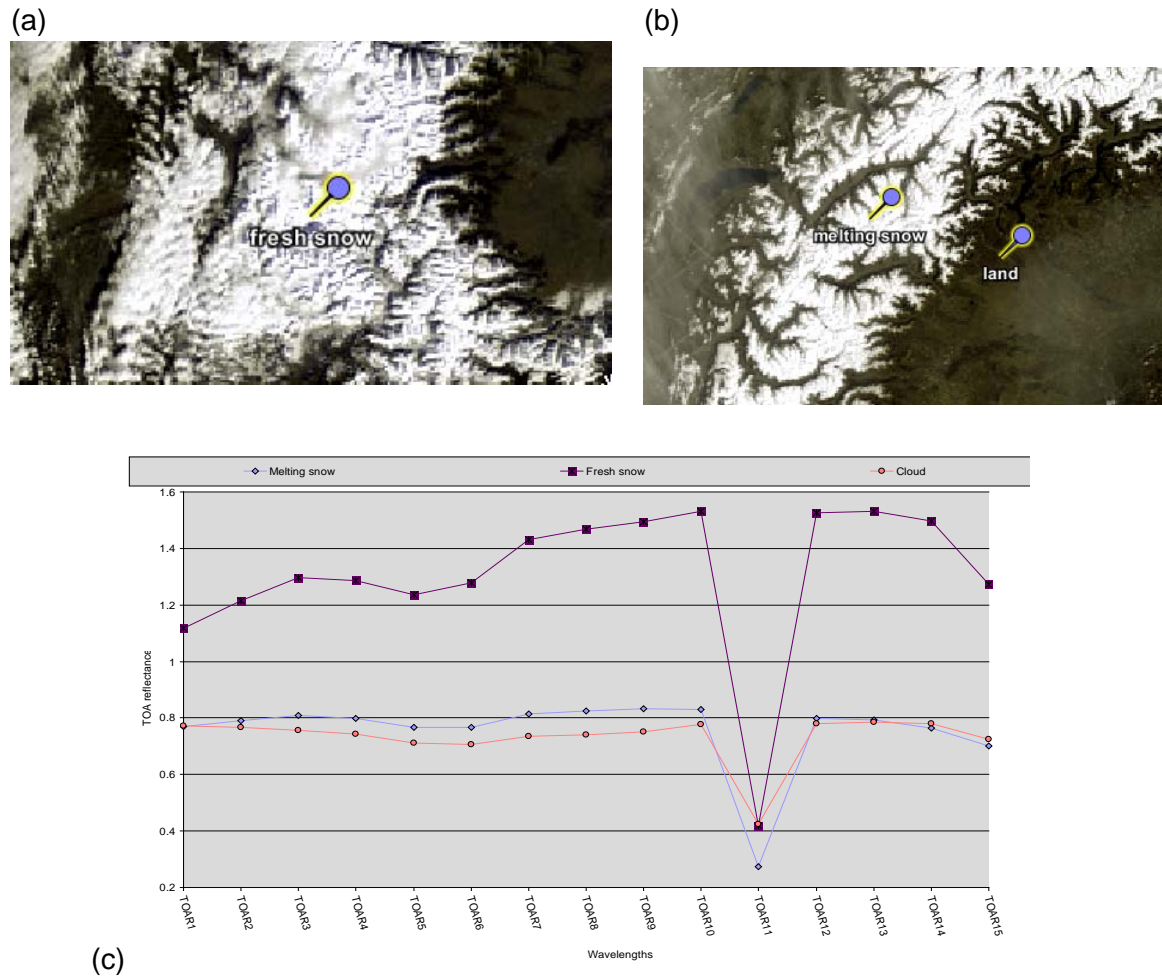


Figure 19: 09 March 2007 MERIS image showing pins for fresh snow and melting snow. The TOA reflectance for the pin locations, fresh snow (violet squares) and melting snow (blue diamonds), plus a typical cloud (orange diamonds)

Table 3 shows the BRR B12/B10 ratio. The differentiation between cloud and snow is difficult to make and the Rayleigh correction is not sufficiently accurate in mountain areas because of the poor spatial resolution of the DEM. Within Table 3 the B10/B1 ratio is also shown to illustrate the

meaningful difference between fresh snow and melting snow; this is out of scope of the classification task, but it may be of potential interest.

Table 3: MERIS spectral ratios for melting snow, fresh snow and cloud

	Melting snow	Fresh snow	Cloud
BRR12/BBR10	0.959	0.996	1.003
BRR10/BRR1	1.082	1.371	1.007

c) **Sand versus cloud:** Two MERIS images over sand were selected; white sand in [Figure 20a](#) and yellow sand in [Figure 20b](#). For both of images, the reclassification of the bright pixels into snow pixels was successful. Two pins were extracted for the TOA reflectance in all the MERIS bands, plus a typical MERIS signal over a cloud. These 3 spectral signatures are plotted in [Figure 20c](#).

[Table 4](#) shows the BRR B12/B10 ratio and that the differentiation between cloud and sand appears quite feasible.

Table 4: MERIS spectral ratio for two types of sand and a cloud

	Libya	White Sands	Cloud
BRR2/BRR10	0.419	0.622	0.990

(a)

(b)



(c)

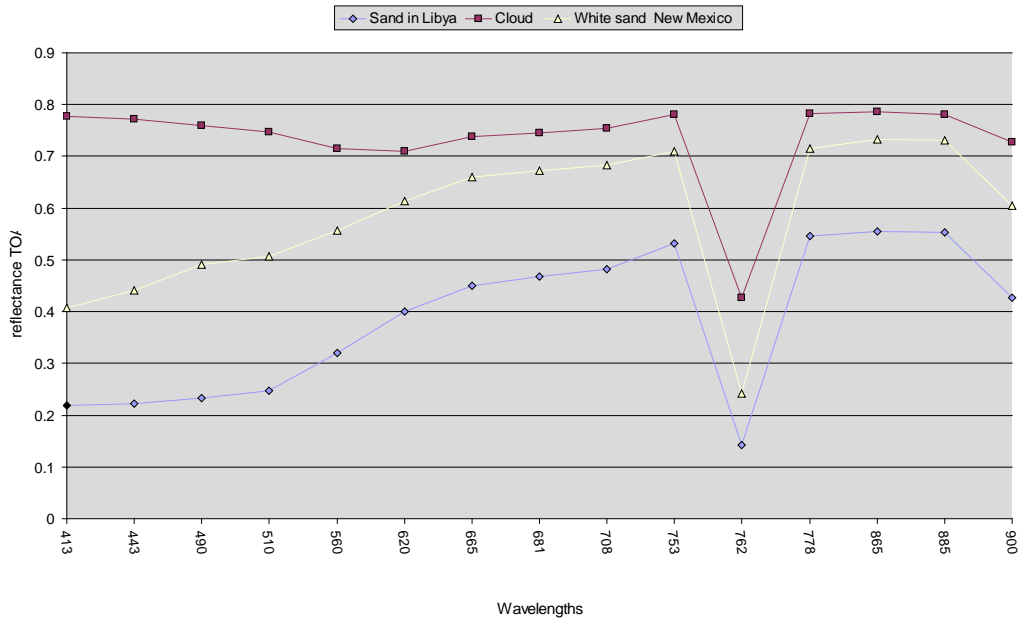


Figure 20: MERIS images showing pins at (a) 12 April 2005 White Sands at 106.20W 32.99N and (b) Libyan desert, 11 January 2005 at 22.5E 26.36N. (c) The TOA reflectance for the pin locations; sand in Libya (blue diamonds), white sand (yellow triangles) and cloud (red squares).

Over water

a) **Cloud versus dust.** The cloud flag threshold was set for a high aerosol loading as severe Saharan dust storms cross the Atlantic Ocean. If, for a cloud, the threshold can clearly separate the bright clouds from the dark ocean, it's certainly not the case for dust plumes; the aerosol loading continuously decreases with the distance from the source. At the transition of the cloud flag, we want to see if the processor raises the quality flags we expect to see. **Table 5** gives the definition of these flags.

Table 5: Definition of MERIS PCDs over water

Identifier	Description
"PCD_1_13"	Uncertain normalized surface reflectance
"PCD_14"	Uncertain total water vapour content
"PCD_15"	Uncertain algal pigment index 1
"PCD_16"	Uncertain yellow substance and total suspended matter
"PCD_17"	Uncertain algal pigment index
"PCD_18"	Uncertain PAR
"PCD_19"	Uncertain aerosol type and optical thickness
"ABSOA_CONT"	Continental absorbing aerosol
"ABSOA_DUST"	Dust-like absorbing aerosol
"ICE_HAZE"	Ice at high aerosol load pixel
"MEDIUM_GLINT"	Corrected for glint

<p>Richard <i>SANTER</i> (LISE)</p> 	<p>SENTINEL-3 OPTICAL PRODUCTS AND ALGORITHM DEFINITION OLCI Level 2 Algorithm Theoretical Basis Document Pixel Classification</p>	<p>Ref: S3-L2-SD-03-C01-LISE-ATBD Issue: 2.3 Date: 17/07/10 Page 38 of 69</p>
--	---	---

"HIGH_GLINT"	High (uncorrected) glint
--------------	--------------------------

A MERIS image was selected, see [Figure 21a](#), with a transect through a dust plume. For the transect, the B13 TOA reflectance plus different flags were plotted; see [Figure 21b](#). A positive flag value indicates that the flag is raised. Between pixels 1 and 20 the cloud flag is raised. Then, PCD_13 and PCD_15 are raised up until the end of the plume (pixel 130). Both are raised again when crossing semi transparent clouds. The ABSOA_dust flag is never raised. A second dust episode is shown in [Figure 22](#). In this case, the cloud flag is never raised along the transect. When B13 is high, PCD_13 and PCD_15 are raised. In between, the aerosol remote sensing module is working with the warning about absorbing dust.

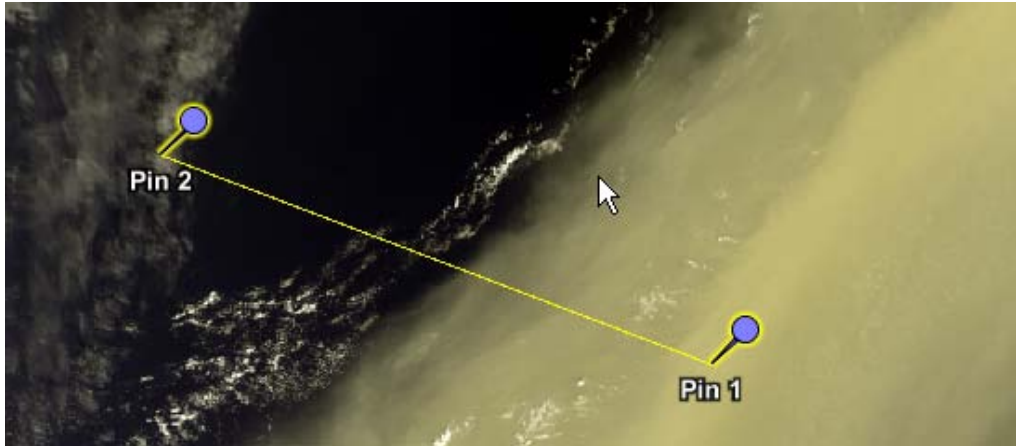
A more detailed analyse requires a more in-depth examination of the level 2 products. However, it can be summarised that the Saharan aerosol events are not correctly identified and processed even if they are of major interest for climatologic studies. However,

- i. The discrimination between cloud and aerosol is possible, based on the spectral signature differences between clouds and aerosols. The differences are visible in the RGB images.
- ii. It is more than relevant to develop a specific aerosol module when this module fails because it *a priori* part of the atmospheric correction.

In other words, the aerosol product over the ocean should be a “real” aerosol product not a “side” product, which is just important for the atmospheric correction.

b) **Cirrus cloud**: Its well know that the MERIS cloud classification is too insensitive: some transparent clouds, mainly cirrus, are not identified. [Figure 23](#) shows a MERIS scene over the British Channel with cirrus cloud. Clearly, PCD_13 and PCD_15 are raised for most of the pixels, including above pixel 170, for which the scene appears to be cloud free.

(a)



(b)

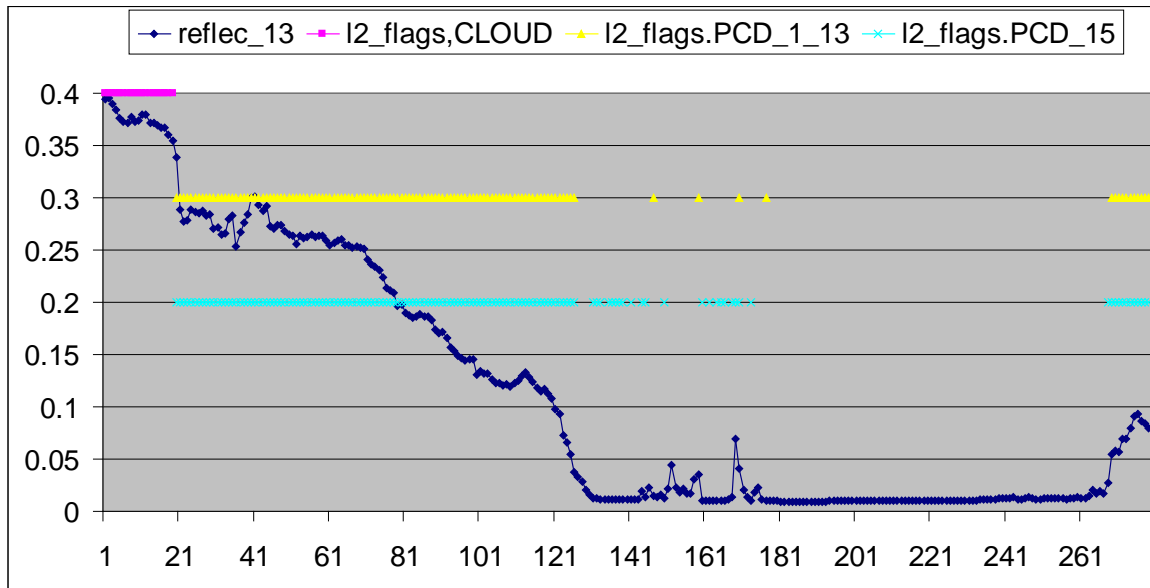
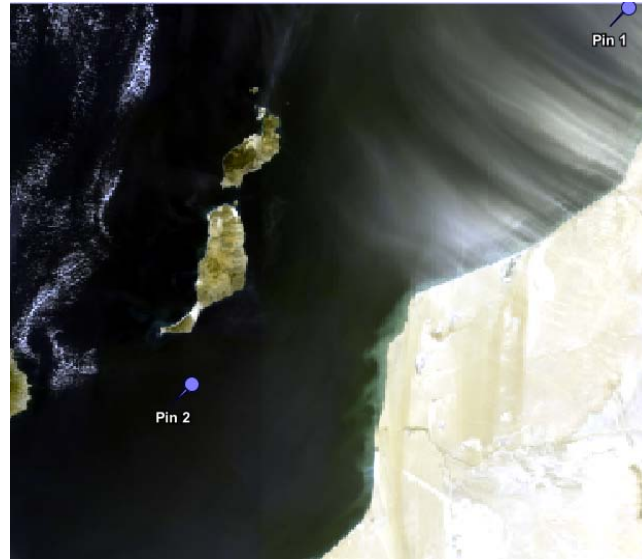


Figure 21: (a) RGB MERIS image of a dust episode, Atlantic Ocean, 06 March 2004. (b) Plot of B13 TOA reflectance and level 2 flags: Cloud flag (pink squares), PCD₁₃ flag (yellow triangles) and PCD₁₅ flag (cyan squares).

(a)



(b)

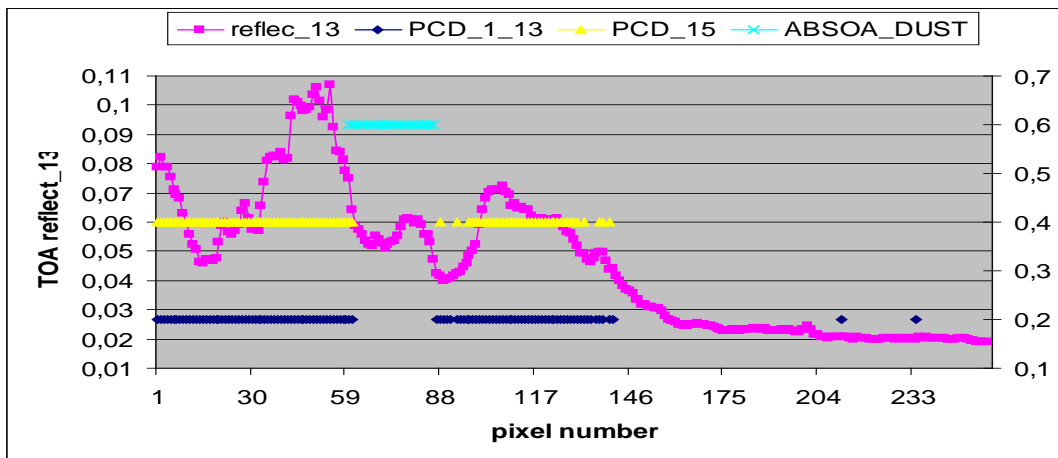


Figure 22: (a) RGB MERIS image of a dust area over Saharan outbreak, 04 November 2003. (b) TOA reflectance (pink squares) scaled on the left axis with Absoa_dust (cyan squares), PCD_13 flag (blue diamonds) and PCD_15 flag (yellow diamonds) appearing only when the flag is raised.

(a)



(b)

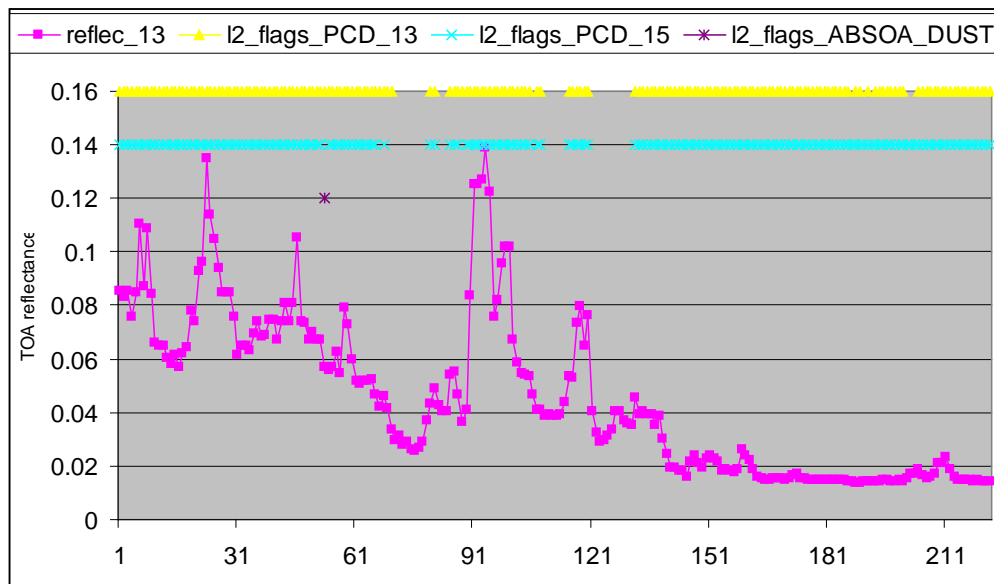
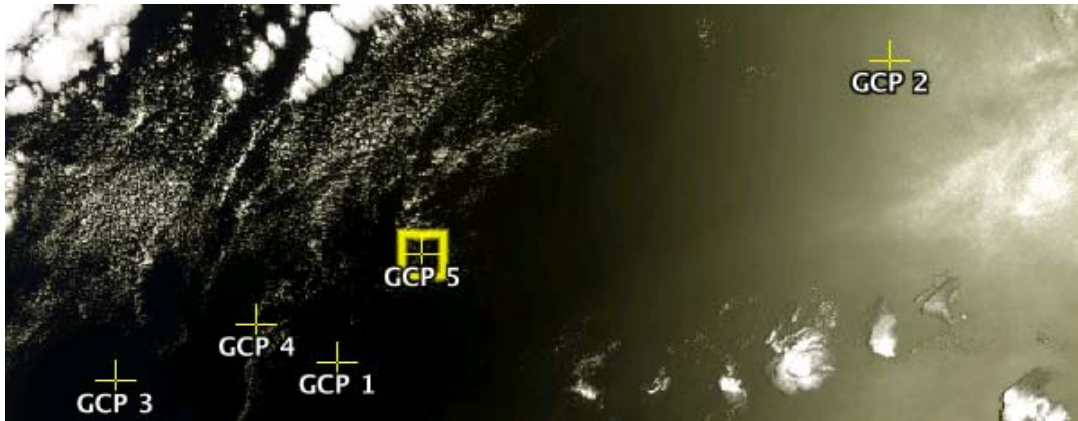


Figure 23: (a) RGB MERIS image of the English Channel, 09 September 2004. (b) TOA reflectance (pink squares) scaled on the left axis with Absoa_dust (violet crosses), PCD_13 flag (yellow diamonds) and PCD_15 flag (cyan crosses) appearing only when the flag is raised.

c) **Glint.** Figure 24 shows the sunglint flags. Along the transect, from P2 to P3, the high sunglint flag is raised up to P5 and the medium glint flag up to P4. The medium sunglint flag is also raised when the high sunglint is raised, which is inconsistent. The end of the medium glint flag corresponds to relatively low reflectance values (less than 2 percent). For another MERIS image, Figure 25, we highlight a strong sunglint. The strong sunglint, because of its brightness, is flagged as cloud.

d) **Radiometric reclassification of water versus land:** We selected, in Figure 26, different situations. B13 and B8 are not corrected from the Rayleigh. The BRR is available at level 2 over the land but not over the ocean. The transect to the French coast is the regular case and we can clearly see the land to sea transition on the B13/B8 ratio. It is even better in the Mouth of the Amazonia River because of the dense vegetation. For Spain, we have bare surface with a small spectral dependence but the differentiation remains. The last scene in the Gulf of Mexico is less favourable for two reasons. First, because the vegetation over land is scarce and the spectral dependence of a bare surface is less pronounced than over vegetated areas. Second, we have a sunglint contamination and the medium sunglint is raised. Over land it appears that the ratio B13/B8 can be below 1. It should be over 1 after the Rayleigh correction. Over the ocean, the ratio is as expected higher in the presence of sunglint. A threshold value at 1 seems to be relevant. Over strong sun glint, B12 will be above B8 but the radiometric classification is not done.

(a)



(b)

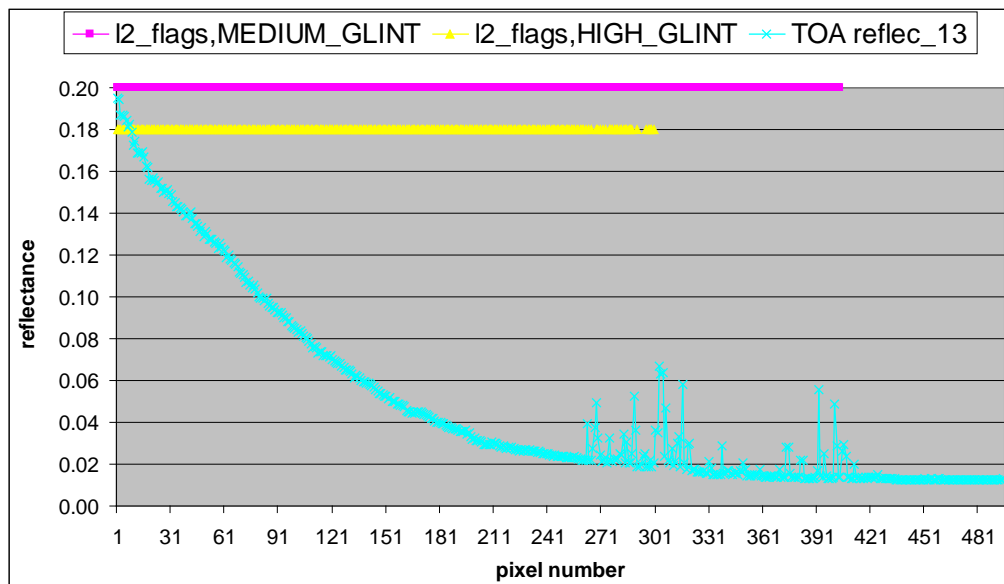


Figure 24: (a): RGB MERIS image of a glint area in the Pacific Ocean, day 2005/05/20, and centre of picture: long: -143.33, lat: 30.11. (b): TOA reflectance (blue cross) scaled on the left along the transect GCP2 to GCP3. Medium glint (pink square) and high glint (yellow diamond) appear when the flag is raised.

(a)



(b)

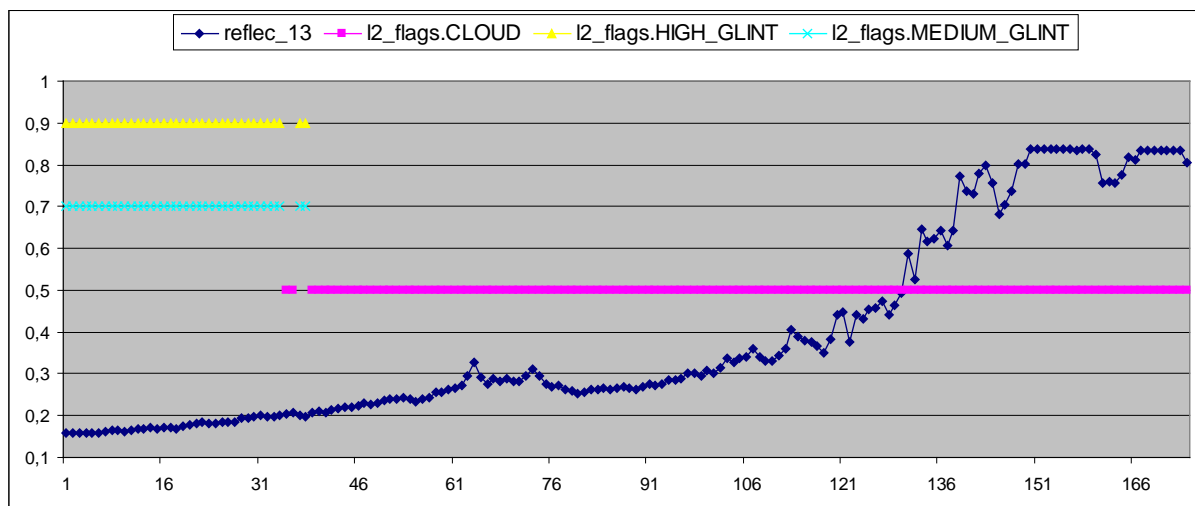


Figure 25: (a) RGB MERIS, Pacific Ocean, day 2005/05/17, long: -144.01W, lat: 22.42N (b) TOA B13 reflectance (blue diamond). And flags: Medium glint (cyan cross), high glint (yellow diamond) and cloud flag (pink point)

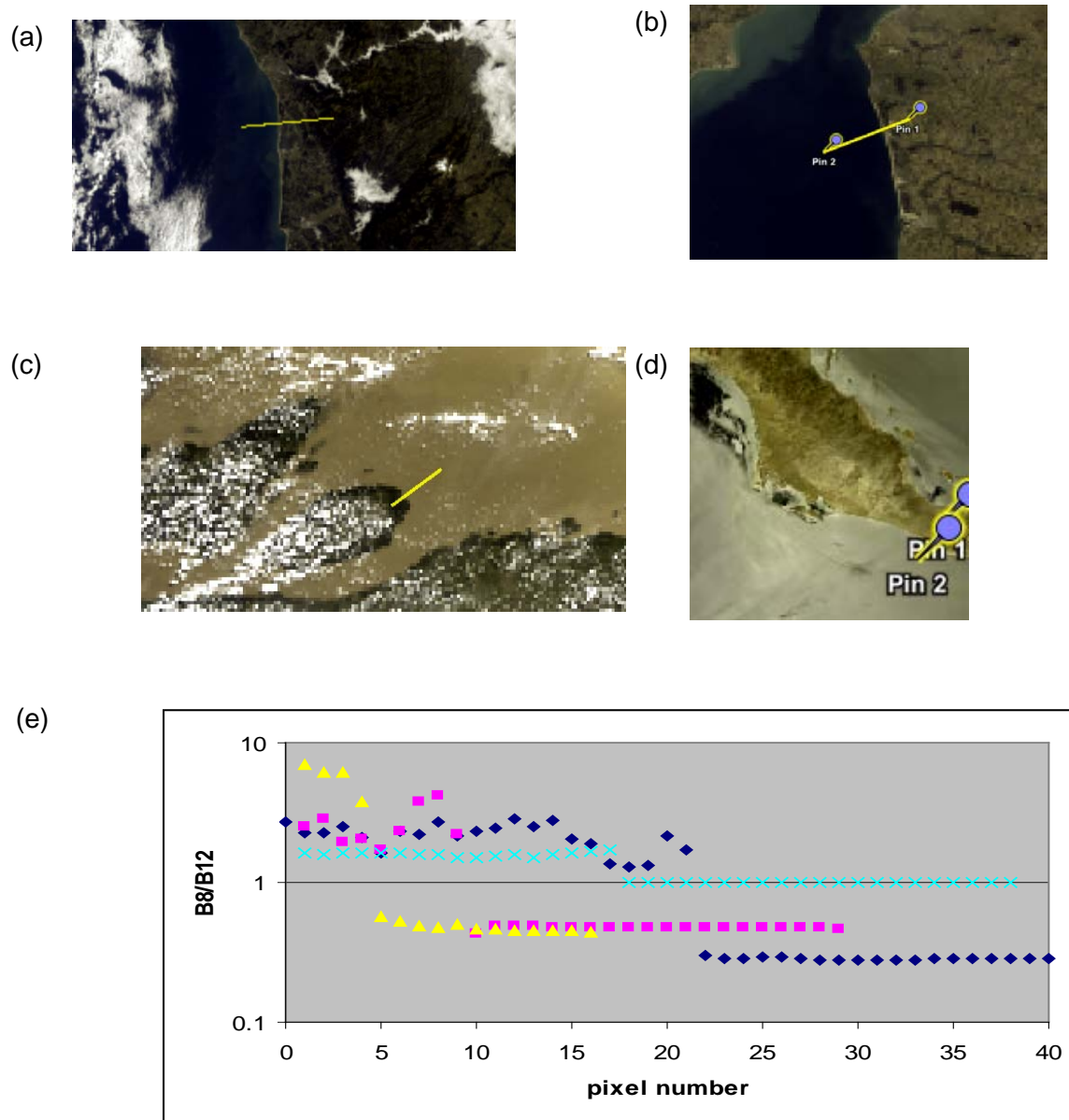


Figure 26: MERIS RGB for (a) Spain on 04 June 2004, (b) English Channel on 09 September 2004, (c) Amazonia on 04 June 2004 and (d) Gulf of Mexico on 04 April 2005. Plots along the transects of (e) Ratio TOA_{B13}/TOA_{B8} with (a) blue diamonds, (b) pink squares, (c) yellow triangles and (d) green crosses for each date.

4.2 MERIS: flags and level 2 geophysical products

Cirrus clouds over land

In September 2004, two consecutive days (8 and 9 September 2004) were selected. On 09 September the meteorological perturbation was coming from the S-W, see [Figure 27a](#), and the level 2 MERIS image is shown in [Figure 27](#); combines the L2 RGB and the cloud flag in yellow. The second RGB for 08 September is also a level 2 RGB, but the cloud flag is never raised.

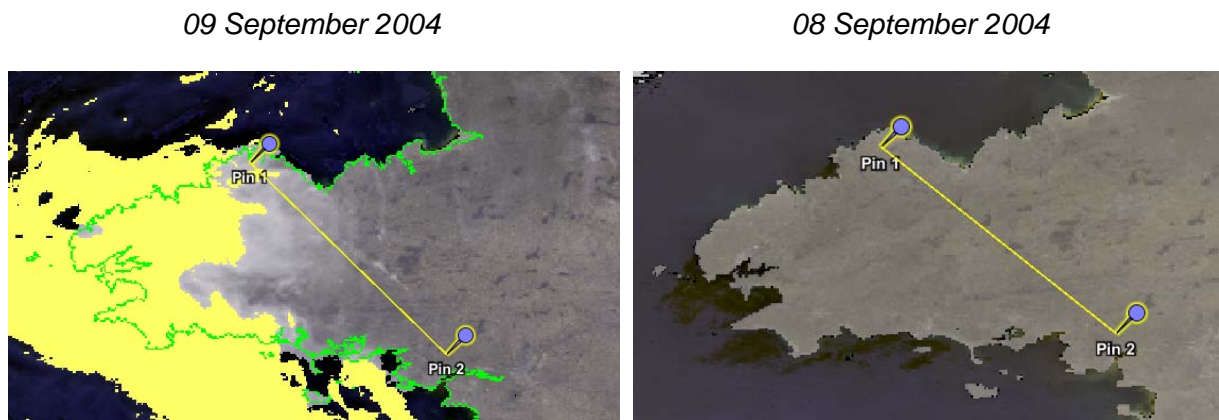
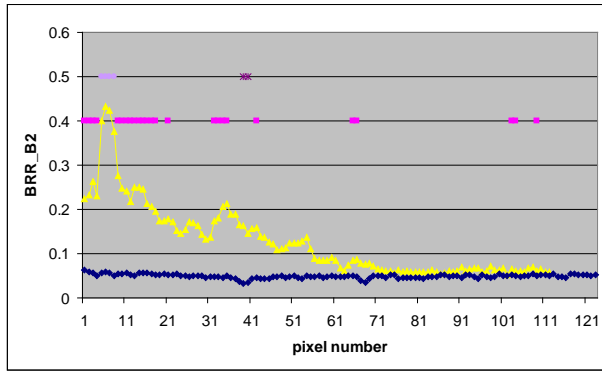


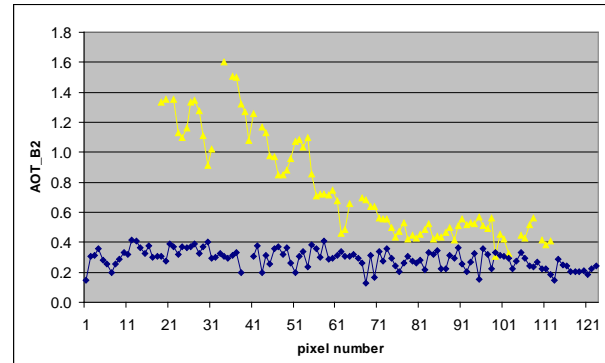
Figure 27: MERIS images over the Britain and France (1.26W 47.85N).

[Figure 28](#) plots different Level 2 products for the two days. [Figure 28a](#) shows the BRR in B2 on which the cloud flag is applied. When raised on 09 September, the cloud flag is arbitrary set to 0.5; it's raised on a few pixels between pixel 5 and pixel 9. The PCD_15, on the MGVI, when raised it set to 0.4. The PCD_15 is also raised on 08 September around pixel 40 and set to 0.5. The AOT_B2 on 09 September, [Figure 28b](#), follows the increase of the TOA reflectance linked to the presence of the cirrus clouds. The MGVI, [Figure 28c](#), appears relatively robust to the presence of cirrus clouds; the PCD_15 is raised when the BRR in B13 goes above 0.2.

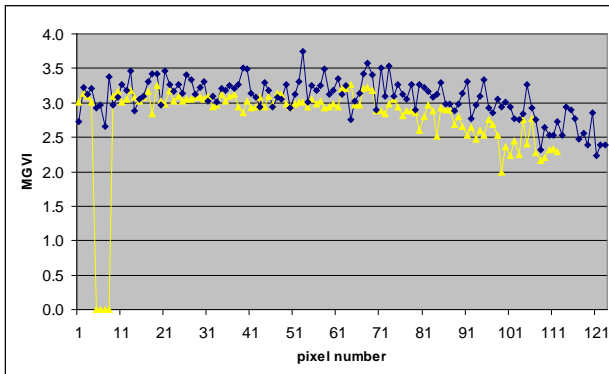
The need for a cirrus cloud flag clearly applies to the aerosol product; the other products seem to be more resistant to the presence of cirrus clouds. A potential cirrus cloud flag should be a quality flag, not a decision flag, and this is discussed in Section 6.2.



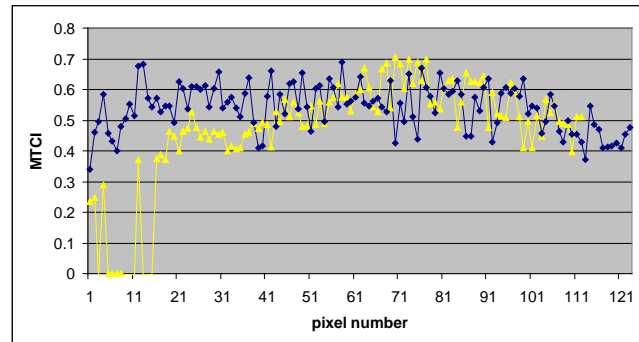
(a)



(b)



(c)



(d)

Figure 28: MERIS L2 product along the transect: (a) BRR_B2 and PCD_, (b) AOT_B2, (c) MGVI, (d) MTCI.

Cirrus cloud over ocean

Reconsidering the MERIS image over the English Channel on 09 September 2004 (see [Figure 17](#)). In [Figure 29](#) a and b the AOT increases in the presence of cirrus clouds while alpha decreases towards 0 to indicate the whiteness of the cirrus clouds. Even if all the PCDs are raised over the cirrus clouds, see [Figure 29c](#), the chlorophyll a determinations (alga_1 and alga_2) appear acceptable; they are similar with no specific discontinuities below the thin cirrus clouds (between pixel number 30 and 100). The end of the transect is more difficult to evaluate.

Dust over the ocean

For the first dust event, Atlantic Ocean on 06 March 2004, the flags re shown in [Figure 30a](#). The AOT, [Figure 30b](#), doesn't follow the dust plume the shape of the TOA reflectance in B13 as it should do. The absence of values up to pixel 80 indicates that the aerosol retrieval algorithm doesn't work in this situation and the PCDs reveal the difficulties encountered.

For different pixels the TOA reflectance was plotted for all the MERIS bands, see [Figure 31](#). The dust appears "yellow" as on the RGB image ([Figure 21](#)). Pixel 1, classified as cloud, should not be and ideally a spectral test (maybe the land sand tests) could be used to identify this pixel as dust rather than cloud.

For the second episode, a Saharan outbreak on 04 November 2003, the dust plume appears thinner and the cloud flag is never raised. The AOT closely follows the shape of the B13 TOA reflectance in B13; see [Figure 32b](#), except when the absorbing dust flag is raised. When this flag is raised (out of scope for OLCI), the discontinuity in alpha is obvious and the relevance of the absorbing dust flag is questionable.

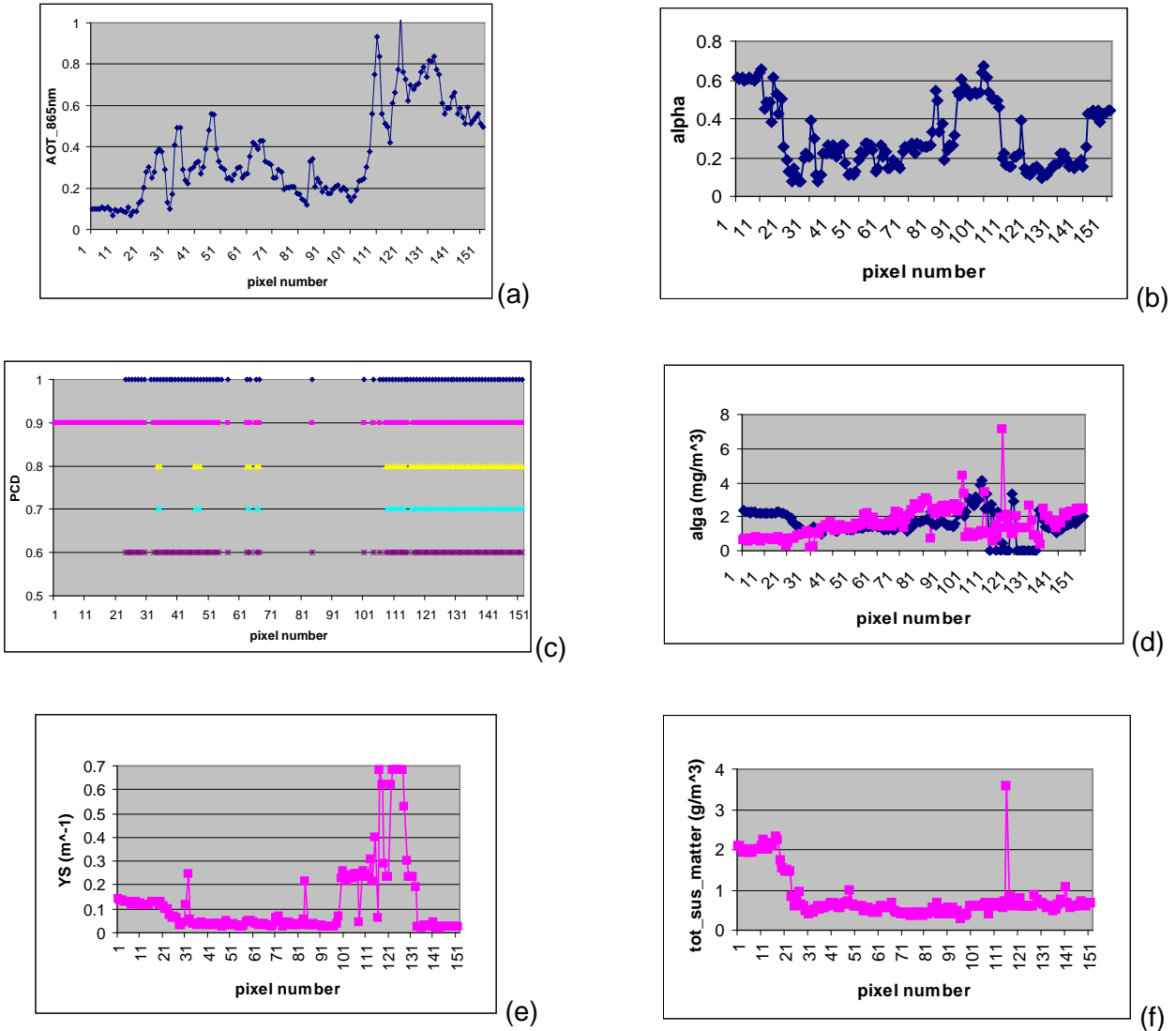
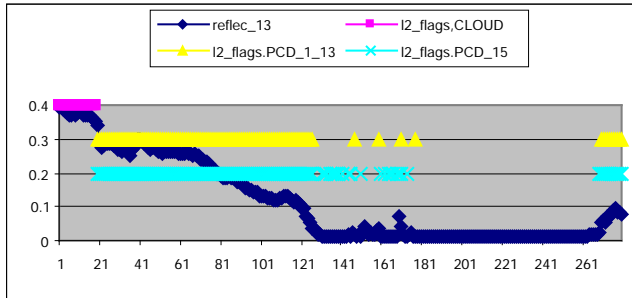
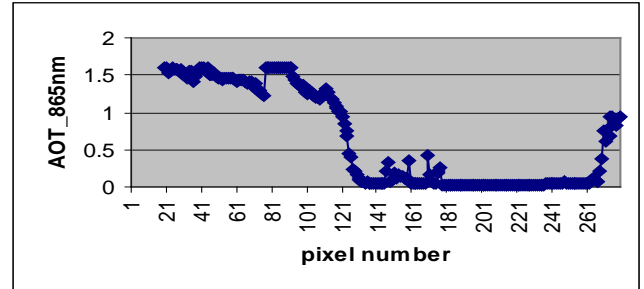


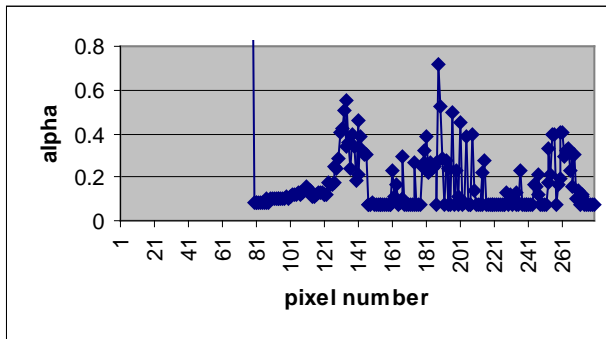
Figure 29: English Channel transect: (a) AOT at 865 nm; (b) Angstrom coefficient; (c) different PCDs: PCD_13=1, PCD_15=0.9, PCD_16=0.8, PCD_17=0.7, PCD_19=0.9; (d) Chlorophyll a content for case 1 algorithm (blue diamonds) and case 2 algorithm (pink squares); (e) yellow substance and (f) total suspended matter.



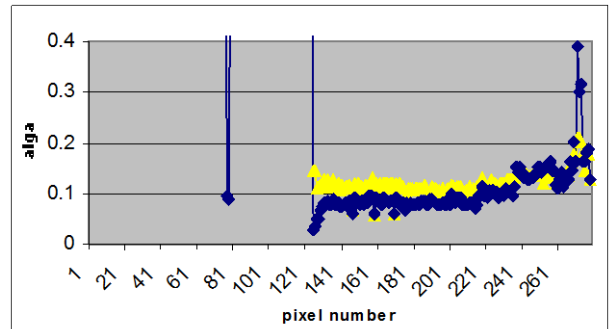
(a)



(b)



(c)



(d)

Figure 30: Transects for MERIS Atlantic Ocean image from 06 April 2004 showing (a) flags; (b) AOT₈₆₅ nm; (c) Angstrom coefficient; (d) alga₁ (blue diamond) and alga₂ (yellow triangle) in $\mu\text{g/l}$.

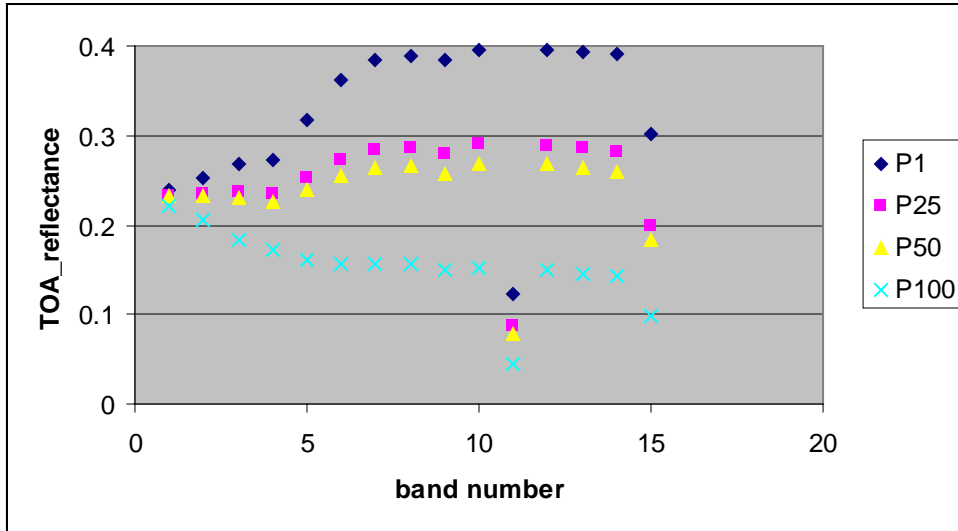
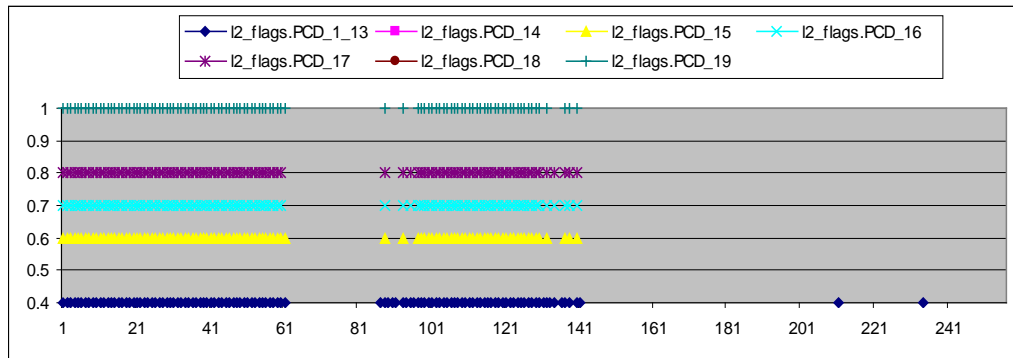
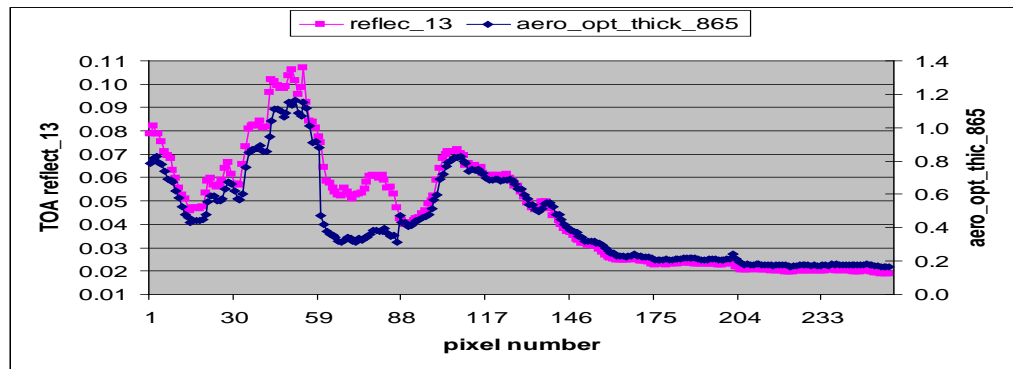


Figure 31: TOA reflectance along the transect at different distances.

(a)



(b)



(c)

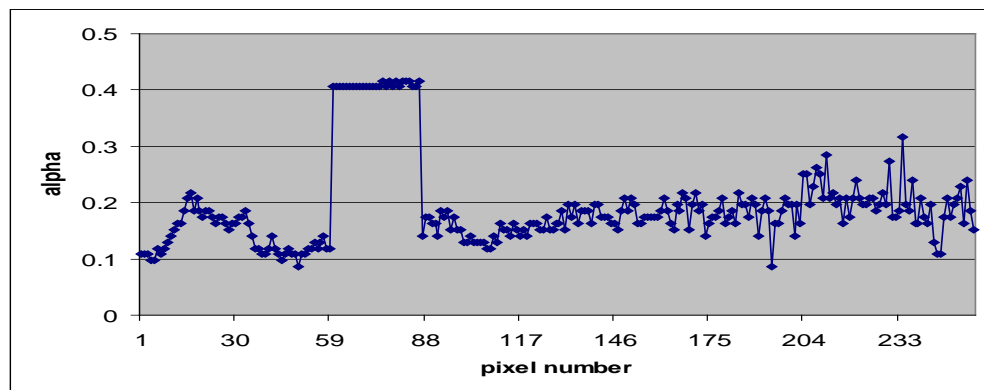


Figure 32: Saharan outbreak on 04 November 2003 with a transect showing (a) flags, (b) AOT and (c) Angstroem coefficient.

Sunglint over ocean

Using the L2 MERIS image acquired over the Pacific Ocean on 20 May 2005 (see [Figure 24](#)). The high sunglint flag is raised at pixel 302 while the medium sunglint flag is raised at pixel 407. When the aerosol product is plotted, [Figure 33](#), the sunglint correction is seen to be overestimated; the aerosol extinction of the direct sunglint is not accounted for and so the AOT artificially decreases while alpha increases slightly because the aerosol extinction is more effective in B12 than in B13. The ocean products shown in [Figure 34](#) seems to be less affected and in this case, the maritime aerosols overestimation is counter balanced by the underestimation of aerosol loading. This favourable case occurs in the open ocean, but not in coastal waters where errors will be larger.

To see the temporal variations in sunglint, three MERIS consecutive images over the Atlantic Ocean were selected. The RGB images are shown in [Figure 35](#) with a visual connotation of the importance of the sunglint. Plotting the transect of the extracted Level 2 flags is shown in [Figure 36a](#). On 07 June all the pixels in the transect were flagged as cloud except for a few pixels after pixel 82 that are flagged as high sunglint. On 06 June 6 all the pixels in the transect were flagged as high sunglint. The 11 June 11 corresponds to a total absence of direct sunglint and the background for the level 2 products is plotted in [Figure 36 b and c](#). The sunglint flags are in line with what is expected for the ocean processing branch, but the confusion between clouds and sunglint is more questionable.

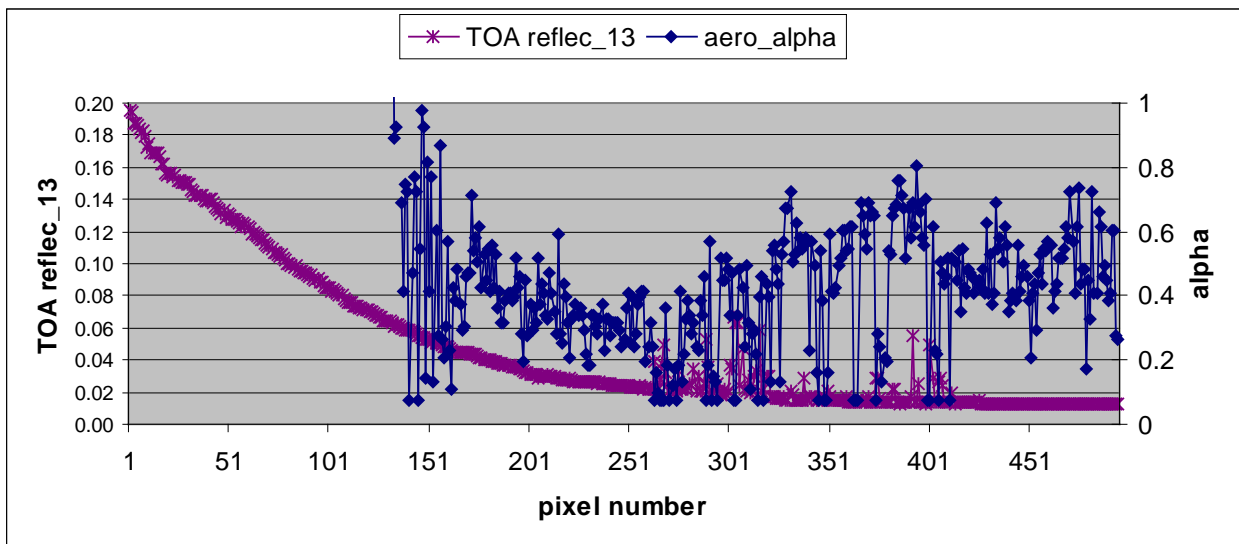
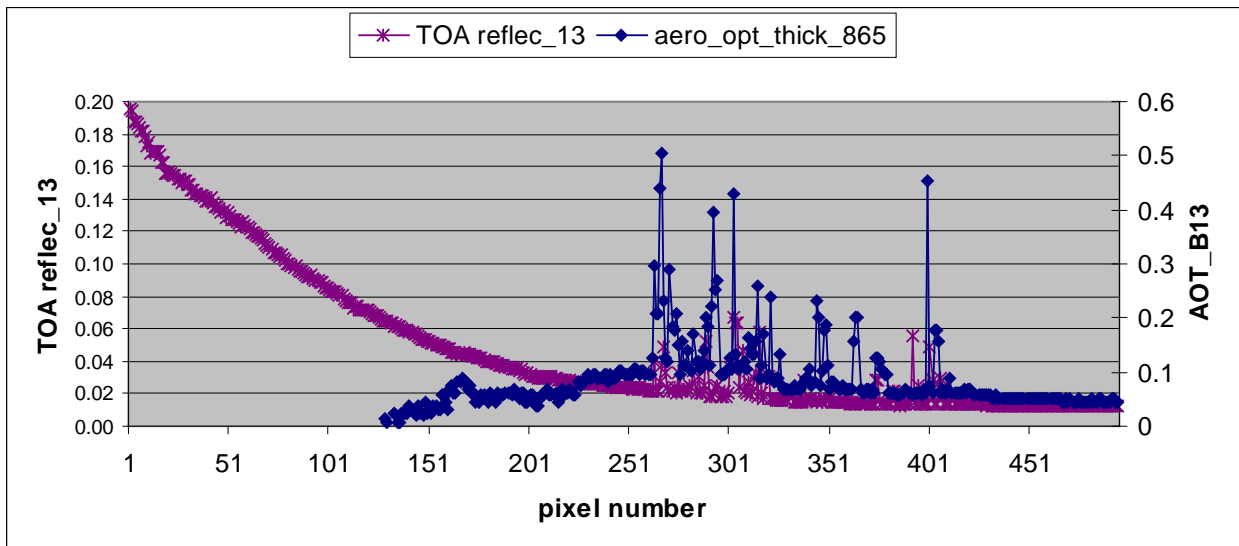
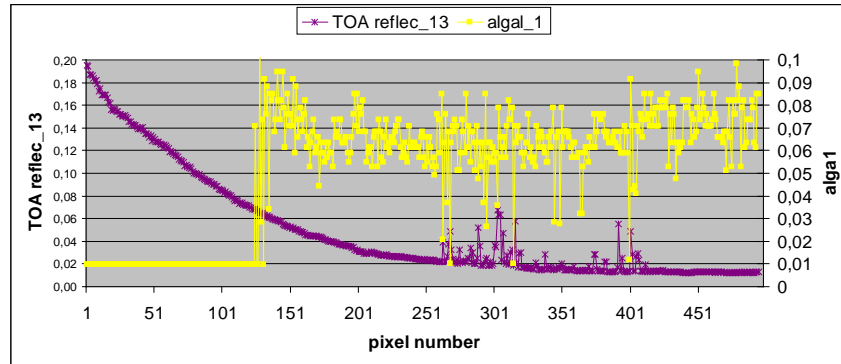
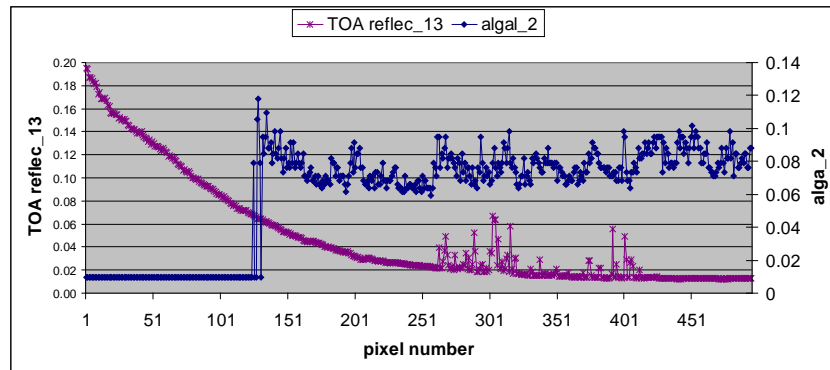


Figure 33: MERIS image over the Pacific Ocean on 20 May 2005 with transects of B13 TOA reflectance and aerosol product (AOT_865 and Angstrom coefficient) plotted.

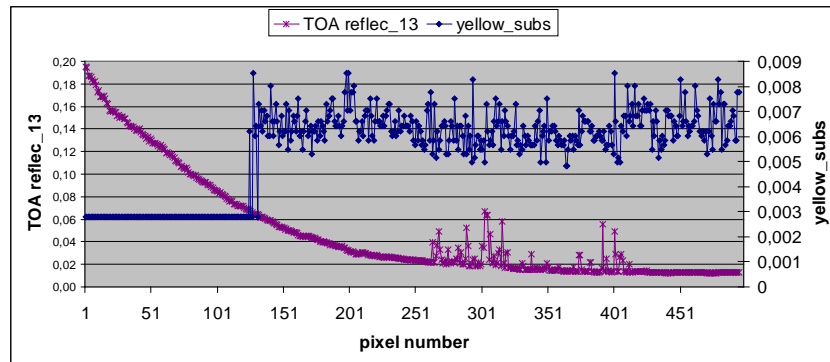
(a)



(b)



(c)



(d)

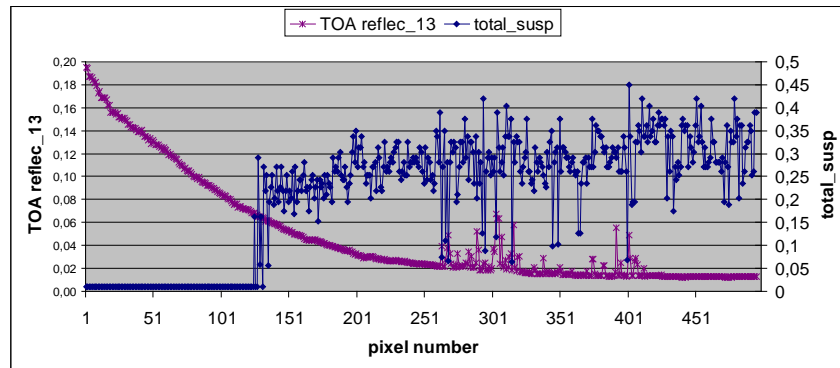
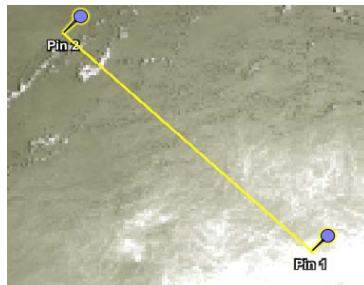


Figure 34: MERIS image over the Pacific Ocean on 20 May 2005 with transects for the TOA_reflectance (violet square) and level 2 products plotted.

Medium glint: 04 June 2004



High glint: 07 June 2004



No glint: 11 June 2004

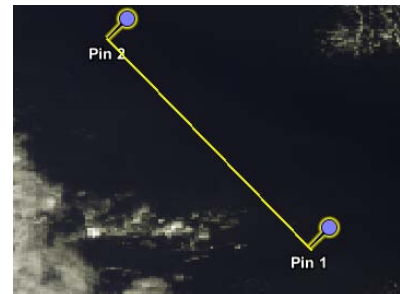


Figure 35: RGB MERIS images over Atlantic Ocean, centre of images are 42.49W 27.80N.

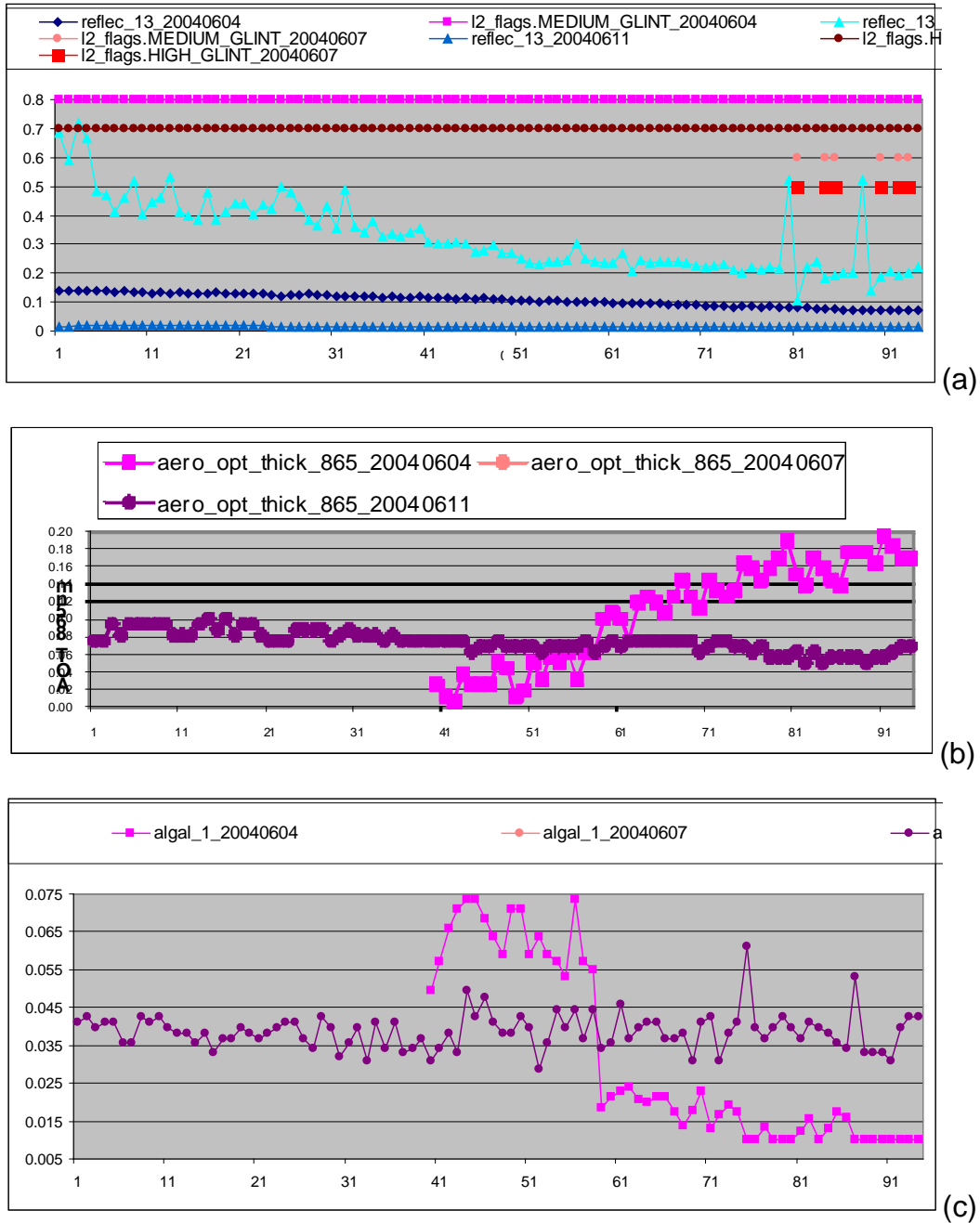


Figure 36: (a) Flags, (b) AOT and (c) chlorophyll a for the MERIS image over Atlantic Ocean.

4.3 Summary of the MERIS Validation and Comment Relevant to the OLCI prototype

In this ATBD, the MERIS level 2 classification was reviewed first. Over land and water, the role of the bright pixel flag is not to detect the clouds but to exclude high signal levels that are not compatible with the performance of the atmospheric processing. It appears to correctly work over land, but over the ocean there is confusion between sunglint and clouds.

A sub classification of the bright pixels over land can be made to distinguish cloud, sand and snow. The sand flag is demonstrated to work (maybe with some difficulties over white sand). It's also recognised that the previous snow test was poorly designed.

Over the ocean, there is more to do over the sunglint area first because of the confusion between cloud and sunglint. Second, the medium sunglint flag (for which a sunglint correction is performed) and the high sunglint flag (for which a sunglint correction is not performed) appear to be quite arbitrary set. For OLCI, there is a separate ATBD dealing with sunglint ().

MERIS L2 products and classification

Simultaneously to the flags, the L2 products were examined. Over land, the bright pixel threshold is well set. The influence of the cirrus clouds directly impacts on the aerosol products, but not the other products. MGVI and MTCI do not appear to be sensitive to the presence of cirrus clouds.

Over the ocean, the presence of the cirrus clouds may alter the products. The absorbing dust flag, at least in one case, was raised in a dust episode. An extensive evaluation of this flag needs to be undertaken.

The situation is more confused in the sunglint. Even in the absence of clouds, the differentiation between medium and high sunglint is quite arbitrary. The L1 glint risk first needs to be revisited and certainly improved. When raised, the sunglint correction should be applied. Then, a L2 glint flag should be raised based on the impossibility to perform a correct atmospheric correction. The threshold values of this flag should result from extensive simulations of the TOA reflectance follows by the L2 process. The control of the retrieval of the aerosol model and of the water leaving radiance is the key to set the threshold.

The land-water radiometric classification based on the ratio B8/B12 works in absence of sun glint. This reclassification in presence on sun glint needs to be re examined.

From MERIS to OLCI

For classification purposes, the MERIS approach is a first guess because the MERIS spectral setting for classification is suitable to S3/OLCI. The band at 1.02 μm is a plus for cloud and snow differentiation. The proposed classification scheme should be first implemented on MERIS and coupled with the geophysical level 2 algorithms and it's a very important concept that we have clear sky rather than cloud flags. The level 1 bright pixels should eliminate the pixels that have no reason to be processed at level 2. However, for geophysical reasons, the processor will re-inject the sand and the snow/ice. During this verification process of the thresholds will be adjusted. It's important to compare on the same scenes and outputs for both the Reduce Resolution (RR) and Full Resolution (FR) modes.

In addition to the overall classification, the impact of the introduction of new spectral bands (mainly 1.02 μm) should be verified.

5. PRACTICAL CONSIDERATION

As cloud screening is not required, because there is no cloud processing branch, the first objective is to achieve the clear sky pixels. Also, over the ocean the aerosol product is only used for atmospheric correction – it's not an atmospheric product and this had an implication on the classification. For MERIS, aerosol remote sensing is conducted even if the atmospheric correction module is not activated for cases of high aerosol loading. However, for OLCI this will not occur. Over the land, we don't need to care about the presence of cirrus clouds as the land products are insensitive to these variations. The bright flag has to be set for the MGVI (or other products), but not for the aerosols.

Over the ocean, the atmospheric correction process starts with the aerosol remote sensing module. The key wavelength is 865 nm. The threshold should be set at 865 nm instead of 442 nm. Rayleigh and gaseous corrections are not needed.

<p>Richard <i>SANTER</i> (LISE)</p> 	<p>SENTINEL-3 OPTICAL PRODUCTS AND ALGORITHM DEFINITION OLCI Level 2 Algorithm Theoretical Basis Document Pixel Classification</p>	<p>Ref: S3-L2-SD-03-C01-LISE-ATBD Issue: 2.3 Date: 17/07/10 Page 60 of 69</p>
--	---	--

6. FUTURE EVOLUTIONS

6.1 Future Evolutions of the MERIS flags

Thanks to the ESA support for various projects, Albedo map (Fischer et al., 2008) and the MERIS O2 project (Santer et al., 2009), an evolution of the MERIS level 2 classification can be envisaged.

Snow-cloud over land

The Normalised Differential Snow Index (NDSI), which exploits the decrease of reflectance from the red or NIR to the medium infra red can be applied. The MERIS Differential Snow Index (MDSI) is uses bands at 865nm and 885nm to simulate the NDSI and has been developed by R. Preusker (FUB) in the framework of the MERIS AlbedoMap project.

$$MDSI = \frac{rho_{toa}(865) - rho_{toa}(885)}{rho_{toa}(865) + rho_{toa}(885)}$$

If a pixel, that has been proven to be bright, has an MDVI > 0.01, then it can be considered as snow or ice; results are reported in (Zagolski et al., 2005). **Figure 37** demonstrates this with a MERIS image over the Alps from 09 March 2009.

With the MNSI, we are dependent on very small effects because the spectral interval between B13 and B14 is small and also we are not in the best spectral arrangement to operate this cloud-snow differentiation. Other possibilities exist and should be investigated:

- i. Water vapour content is small in the cold air over snow compared to over cloud.
- ii. O₂ derived surface pressure.

(a)



(b)

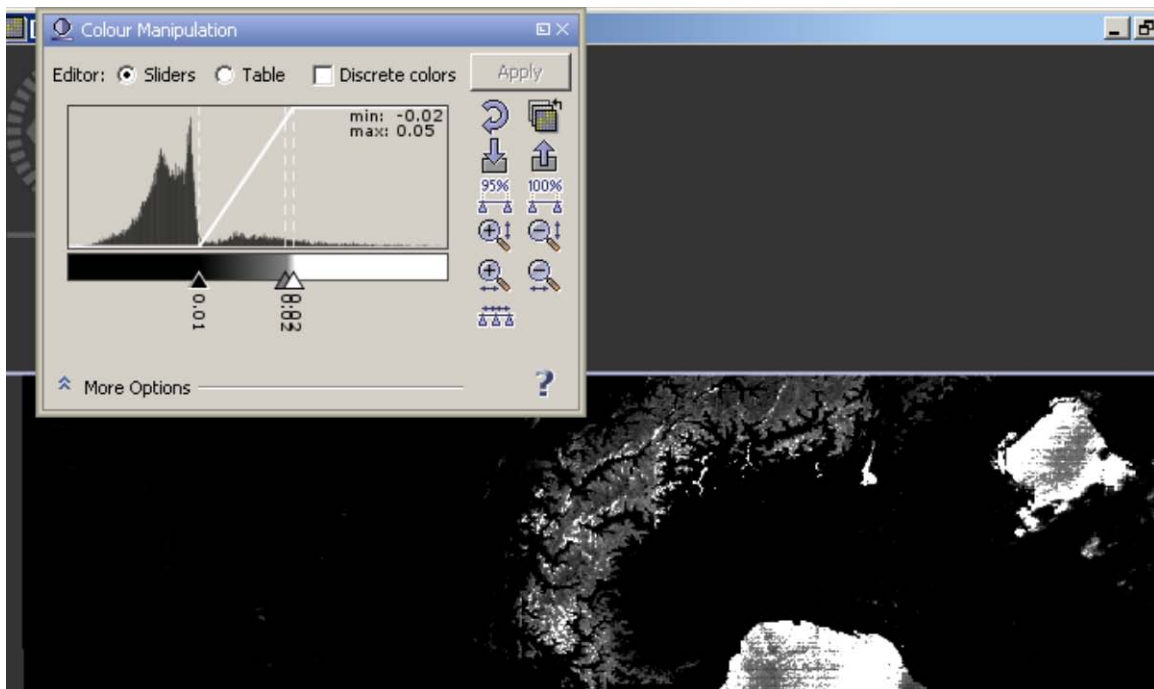


Figure 37: (a) RGB MERIS image from 09 March 2007 and (b) resulting MNSI.

The O2 pressure and the cirrus flag over land

One possible output of the oxygen project is the apparent pressure of the land-atmosphere system, P1. Using a transect from a MERIS image acquired over the Brittany in France on 09 September 2004, see [Figure 38](#), there is a clear relationship between the P1 pressure product and the AOT.

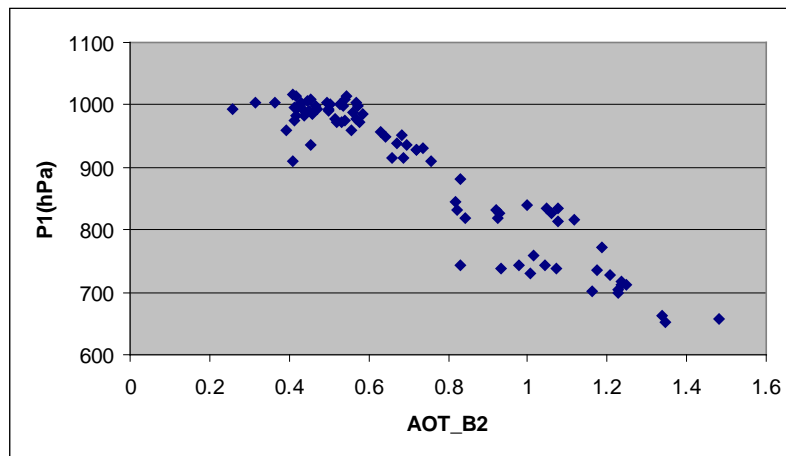


Figure 38: Apparent pressure (P1) plotted against AOT at 443 nm for MERIS transect across French Brittany on 09 September 2004.

The O2 pressure and the cirrus flag over water

One possible output of the oxygen project is the apparent pressure P_{scat} of the scatters (aerosol or thin clouds). A transect over the MERIS image over the British Channel acquired on 09 September 2004 demonstrates a clear relationship between this P_{scat} pressure and AOT, see [Figure 39](#).

If there is strong information on the presence of the cirrus clouds, thanks to the oxygen band, it is difficult to use a binary flag to exploit this information. A threshold can be set where there is a close relationship with the tolerance to errors within the level 2 products; in particular the aerosol product. Therefore, a binary flag can only be a quality flag and not a decision flag. Therefore, Instead of a binary flag it's more relevant to develop an index risk of the presence of cirrus clouds scaled between 1 and 8.

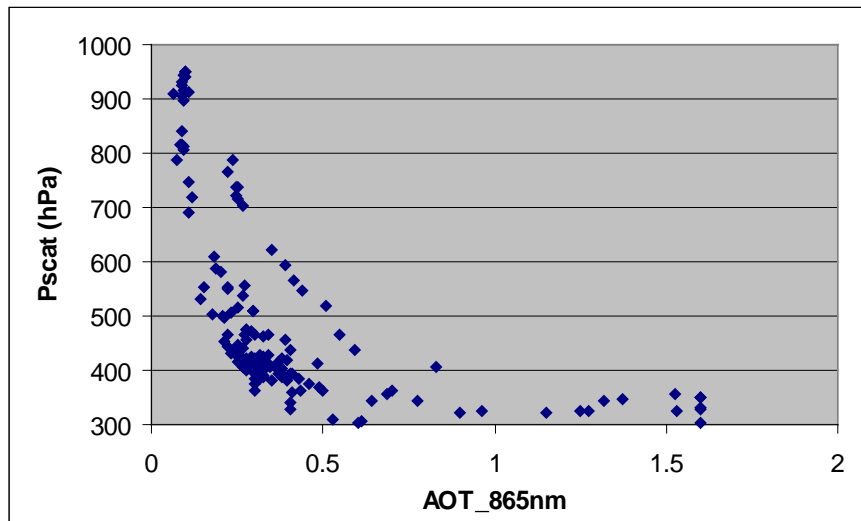
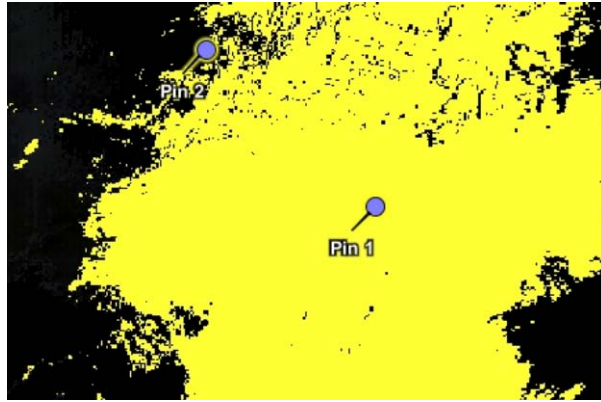


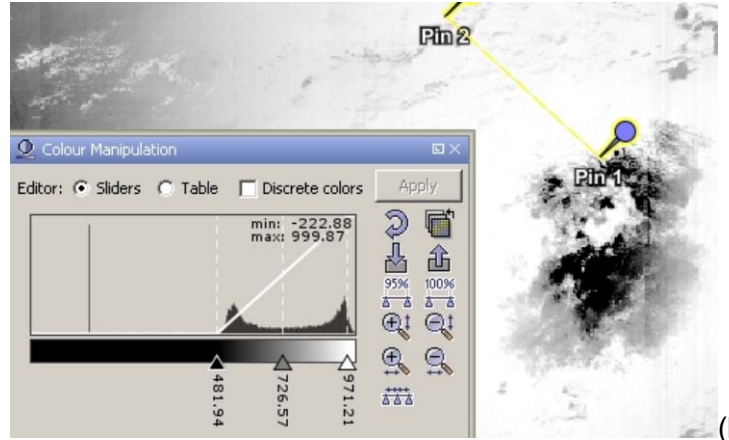
Figure 39: Apparent scatter pressure (P_{scat}) versus AOT at 865 nm plotted for a MERIS transect across the British Channel on 09 September 2004.

The O2 pressure and the cloud identification over sunglint

For the sunglint scene collected on 07 June 2004 over the Atlantic Ocean (see Figure 35), the L2 cloud flag was wrongly raised on the transect and over the sunglint spot. On this image, Figure 40a, the cloud flag is systematically raised over the sunglint. If we plot the O2 P1 pressure (see Figure 40b), as expected, over the sunglint the pressure is close to the sea level pressure. Cirrus clouds appear in the vicinity of pin 1 and P1 is complementary to the cloud flag in the upper left corner of the image. Complementary to that, thin cloud can also be detected over the sunglint thanks to P1.



(a)



(b)

Figure 40: Sunlint over the Atlantic Ocean on 07 June 2004 with (a) L2 cloud mask shown and (b) O2 derived pressure plotted along a transect.

<p>Richard <i>SANTER</i> (LISE)</p> 	<p>SENTINEL-3 OPTICAL PRODUCTS AND ALGORITHM DEFINITION</p> <p>OLCI Level 2 Algorithm Theoretical Basis Document Pixel Classification</p>	<p>Ref: S3-L2-SD-03-C01-LISE-ATBD Issue: 2.3 Date: 17/07/10 Page 65 of 69</p>
--	--	---

6.2 Quality flags (indices) for the atmosphere

Over the Land

Atmospheric indices can be defined on demand:

- i. A high aerosol loading; this index is not a decision flag for OLCI because the atmospheric branch is de-scoped.
- ii. A cirrus cloud index.

Over the Ocean

The following flags are possible atmospheric quality flags; raised for atmospheric issues. In reality, it's more relevant to define quality indices (not binary i.e. not yes or no) rather than flags for three reasons: it doesn't need to be binary; it's an opinion of continuous parameters; a quality index can be used to weight spatial and/or temporal averages in the generation of product of upper levels. The following quality indices are possible:

- **Cirrus cloud index:** As already mentioned in Section 6.1, P_{scat} can be converted into this CCI.
- **Cloud vicinity index:** [Figure 41](#) is a RGB MERIS image where a transect from water to clouds (pin4 to pin5) is selected. [Table 6](#) reports the level 2 for the "clear" sky pixels. The aerosol optical thickness slightly increases and the aerosols become a little whiter. The alga indices are not very sensitive.

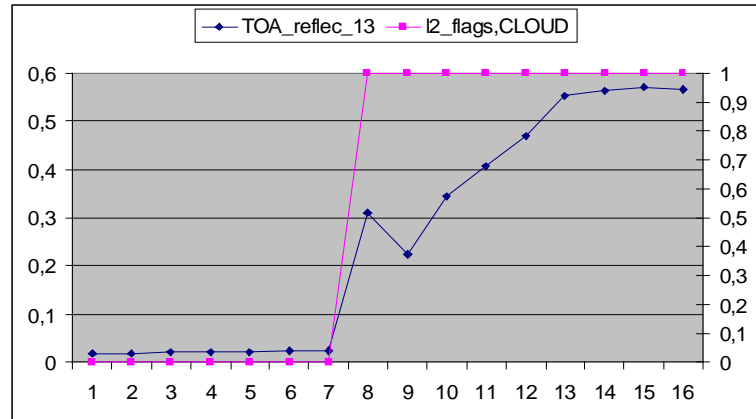


Figure 41: (left) RGB MERIS image over the Portugal Coast: (12.94W 43.37N) on 07 September 2006. (right) B13 TOA reflectance and L2 flags (CLOUD) along the transect.

pixel number	algal_1	algal_2	aero_alpha	aero_opt_thick_865
1	0.152	0.136	0.824	0.076
2	0.169	0.146	0.857	0.076
3	0.157	0.114	0.946	0.082
4	0.152	0.136	1.034	0.082
5	0.146	0.114	1.045	0.094
6	0.163	0.118	0.957	0.113
7	0.163	0.118	0.968	0.120

Table 6: Chlorophyll and aerosol products in the vicinity of a cloud.

7. ASSUMPTIONS AND LIMITATIONS including ERROR BUDGET

7.1 Reconsidering the role of the flags

When there is a bright cloud over water, the flag setting is straightforward. The difficulty is to set a flag for an ambiguous pixel. Here, two overall considerations should be kept in mind:

- **OLCI** level 2 algorithms are restricted to the production of surface reflectance (and to associated geophysical products).
- An error bar (or a quality indicator) should be attached to the level 2 products.

The first consideration invites us to re-examine the need to maintain some of the atmospheric algorithms. Do we really need to have O₂ derived surface pressures for the classification? We will have two spectral OLCI bands in the O₂ absorption around 761 nm, which we can use directly with the TOA radiance (or reflectance) in these two bands to improve the classification. Over land, do we still go for a Rayleigh correction for the level 2 product? If not, how will it change the classification process over land?

The classification was conceived from the top (TOA radiance) to the bottom (Level 2 products), but could be thought of in a reversed way... at least to set the thresholds i.e. we raise a flag where the error bar on the level 2 geophysical product is above the specifications. Therefore, the setting of the threshold for ambiguous pixels consists in applying the level 2 algorithms (on synthetic or measured values) and identifying the situations for which the outputs do not meet the specifications.

7.2 Binary flag or geophysical information

Some flags are by essence binary: land or water, bright cloud or not. Some of them are raised correspond to a continuous influence of an invisible contributor e.g. sunglint and cirrus clouds.

If a flag is binary, an error budget can be only conducted with a statistical approach that associates the flag to a level 2 outputs (product or flag) through a quality assessment of this level 2 product.

In the cases where we define the threshold versus the robustness of the algorithm to their presence, then the use of a non-binary flag may be better. As an example, the impact of the presence of the cirrus clouds is noticeable in the O2 derived pressure. It's difficult to set a flag on a factor (the presence of cirrus clouds), which has a continuous effect on the products because the threshold depends on the product itself. It's the case over land, for which we need to account for the presence of the cirrus clouds in the examination of the aerosol product; not for the MGVI. The situation is even more confused over water. Therefore, instead of a flags the relevant O2 pressures could be used as an auxiliary parameter to a given algorithm, which would:

- i. Improve the product: The aerosol remote sensing and atmospheric correction can use an O2 pressure for improvements.
- ii. Set a decision flag for this specific algorithm.
- iii. Define a quality index for this specific algorithm.

If the maturity of such approach is not high enough, the O2 derived pressure should be a product and the documentation should help the user undertake a quality assessment.

8. INPUT DATA

Inputs are:

- Level 1 inputs i.e. TOA reflectances and flags (bright, land_water and glint risk flag)
- LUTs for the classification atmospheric correction; could be derived separately as described in Section 3.2 (*Threshold for case 1 water, TM1B*) or use the Atmospheric Correction LUTs (see ATBD SD-03-C07) which would be more consistent.

9. REFERENCES

Bourg, L., et al., 2009, MERIS Level 2 Detailed Processing Model, Issue 8.0; PO-TN-MEL-GS-0006, 15 July 2009.

Cox and W. Munk, 1954, Measurement of the roughness of the sea surface from photographs of the sun's glitter, *J. Opt. Soc. Am.*, 44: 838–850.

Deuzé, J.L., Herman, M. and R. Santer, 1989, Fourier series expansion of the transfer equation in the atmosphere-ocean system, *J. Quant. Spectroscop. Radiat. Transfer*, 41 (6): 483-494.

Fischer, J., Preusker, R., Muller, J-P., Zühlke, M., Brockmann, C., Krämer, U., Eskelonen, M. and P. Regner, 2008, Albedo map MERIS global land surface albedo maps. MERIS AATSR workshop, ESRIN. <http://earth.esa.int/cgi-bin/confm8.pl?abstract=209>

Montagner F., Billat V. and S. Bélanger, 2003, MERIS ATBD 2.13, Sun glint flag algorithm, 10 June 2003. http://envisat.esa.int/instruments/MERIS/atbd/atbd_2_13.pdf

G. Moore and S. Lavender, 2010, Case 2 (S) Bright Pixel Atmospheric Correction, MERIS ATBD 2.06. http://envisat.esa.int/instruments/MERIS/pdf/atbd_2_06.pdf

Santer R. and C. Brockman, In Press, MERIS Pixel classification, ATBD 2.17.

R. Santer et al., 2009, ATBD pressure over the ocean, ESA Project: Exploitation of the O2 absorption band. Internal report.

K. Stamnes et al, 2007, ADEOS-II/GLI snow/ice products — Part I: Scientific basis, *Remote Sensing of Environment*, 111: 258–273.

Zagolski F., Aubertin G., J.F. Leroux and G. Péron, 2005, Specification of the Scientific Contents of the MERIS Level 2 Auxiliary Data Product, BOMEN report, PO-RS-BOM-GS-0002, 30 Nov 2005.